Surface Modification of Poly(ethylene terephthalate) (PET) for Effective and Regenerable Microbial Protection

By

Nan Zhao

July 20, 2010

A Thesis
Submitted to the Faculty of Graduate Studies Partial Fulfillment of the Requirements
for the Degree of

Master of Science

Department of Textile Sciences

University of Manitoba

Winnipeg, Manitoba

Abstract

Publics are facing a great challenge of infections from pathogens, most significantly from multidrug-resistant bacteria in healthcare facilities. Textiles are susceptible to contamination of various microorganisms and contaminated medical use textiles can be important sources of cross-infections. Polyethylene terephthalate (PET) is widely used in health-care settings as surgical gowns, protective drapes and privacy curtains. Therefore, it is vital to research and develop effective and regenerable antimicrobial PET fabrics.

In this study, effective antibacterial modification of PET was achieved by immobilizing N-halamine biocide poly(N-chloroacrylamide) (PCA) onto PET through the formation of a surface interpenetrating network. The successful and uniform immobilization of polyacrylamide (PAM) on PET was confirmed by FTIR and XPS. The immobilization is durable to a 72 hours soxhlet extraction. Surface morphology of the fabrics did not significantly change after modification until the immobilization percentage exceeded 20%. The modified fabric can bring 100% reduction of 10^6 CFU/ml of several clinical important bacteria in 15 min contact. The regenerability of N-halamine on PAM modified PET with three different crosslinkers were studied by FTIR, titration and N analysis. It was found that breaking down of the PAM network in chlorination accounted for the loss of regenerability. After 30 regeneration cycles, the PAM-DVB network modified PET was still able to provide 100% reduction of HA-MRSA in 20 min contact. The amount of immobilized N-halamine on PET could be controlled by adjusting irradiation duration, swelling duration, monomer concentration, crosslinker species and initiator, crosslinker concentration. Furthermore, the modification could keep the interspaces between fibers and good breathability of the fabrics.

Acknowledgement

The author wants to express her genuine thank-you to her advisor, Dr. Song Liu, for his wise guidance and patient training and encouragement throughout the study.

Also special thanks are expressed to Dr. Michael Freund, Department of Chemistry and Dr. Wen Zhong, Dr. Lena Horne and Dr. Tammi Feltham, Department of Textile Sciences for their professional assistance and expert advice.

The author is also grateful for the financial support from the Manitoba Medical Science Foundation (MMSF) grant, the Natural Sciences and Engineering Research Council of Canada (NSERC) Discovery grant, and the start-up fund from University of Manitoba. Special thanks go to Dr. Michael Freund for providing access to the XPS facility in the Manitoba Regional Materials and Surface Characterization Facility at the University of Manitoba.

The helps from Dr. George Zhanel, Department of Medical Microbiology are also appreciated for providing the bacteria in the study.

Finally thanks to my family, friends and colleagues for their consistent help and support. Without them I could not finish my study.

TABLE OF CONTNETS

List of Tables:

List of Figures:

Chapter 1: Introduction

People nowadays are generally aware of the problems associated with microbial contamination in healthcare facilities especially in hospitals. Infectious diseases have become a critically important global healthcare issue which may cause great loss of money and human lives. With the increasing occurrences of antibiotic resistant bacterial strains and community-type outbreaks, textile materials have become one of the major sources of cross-infections in hospitals and medical institutions. Poly(ethylene terephthalate) (PET) is now widely used as reusable protective textile in hospitals because of its good mechanical properties, durability and reusability, thermal stability, ease of processing and its low production cost.(Yang & Kim, 2008)The production and consumption of reusable PET in medical application such as scrub suits, lab coats and privacy drapes increased continually in recent years as reusable textiles raised attention. However, PET is susceptible to contamination of many microorganisms including bacteria, viruses and spores some of which can survive as long as 90 days on PET (Neely & Maley, 2000; Neely, 2000; Neely & Orloff, 2001), so the contaminated PET can serve as an important medium for infectious diseases. To decrease the possibility of cross-infection, it is necessary to introduce antibacterial property/function to PET surface. N-halamine was adopted in the project as antimicrobial agent to be immobilized on PET for its effective and regenerable antimicrobial function which fits well with the reusable protective application of PET in healthcare facilities. However chemical modification of PET is challenging because of its inherent chemical inertia characteristic, high crystallinity and hydrophobicity. Thus many people commit themselves to the researches of durable and regenerable antimicrobial PET.

Chapter 2: Objectives

The principle purpose of the study is to develop reusable antimicrobial PET for medical applications such as nurse uniforms, surgical gowns and protective drapes, etc.

The specific objectives are:

1. To establish and optimize the modification method to produce PET efficiently modified with acrylamide.

2. To obtain antimicrobial PET by chlorination following the immobilization of amide groups and evaluate the antibacterial performance of PET modified with N-halamine.

3. To investigate the regenerability of antibacterial performance of PET modified with N-halamine and the factors which will influence the performance.

Chapter 3: Literature review

This literature review addresses the major problem of nosocomial infection, antimicrobial agents used in textiles, introduction of polyester and its modification methods, and the test methods of antimicrobial efficacy.

3.1 Nosocomial infection

Infections acquired during a hospital stay are called nosocomial infections. Formally, they are are defined as infections arising after 48 hours of hospital admission. Nosocomial infection has become a serious concern for the healthcare community. 2 million new cases of hospital acquired infections occur annually leading to 90,000 deaths and 5 billion dollars of added healthcare costs in the U.S. alone (Gregory, Ahmad, Madkour & Gregory, 2007). Neely and his colleagues studied the survival of microorganisms including gram-positive bacteria, gram-negative and fungi on various common hospital textiles. The research showed that at original concentration of 10^4 to 10^5 CFU/ml per swatch, bacteria and fungus could survive at least 1 day and some of the gram-positive bacteria even stayed alive for more than 90 days. Until now many Gram-positive organisms as MRSA, VRE and Streptococcus pneumonia and medically important fungus as Candida spp. have been reported antibiotic resistant. What's more, the development of resistance is alarmingly progressive (Gregory et al.; Neely, 1999; Millar et al., 1994). Contaminated materials serve as one of the major sources of cross infection. Soil, dust, solutes from sweat and some textile finishes can all be nutrient sources for microorganisms helping to their survive (Purwar & Joshi, 2004). The survived bacteria on textile surfaces could be easily re-dispersed to people around. Therefore, the introduction of biocidal functions into a target material is an effective method to

deactivate the microbes and thus decrease infection, particularly as antibiotic resistance increasing. In addition, through antimicrobial treatment, textiles can achieve better wearing comfort by avoiding undesired odor (Bender & Peter, 2001).

3.2 Antimicrobial agents used in textiles

To win the battle against nosocomial cross infection, introduction of antimicrobial functions to textiles used in healthcare facilities is a very effective strategy.

3.2.1 Introduction of antimicrobial agents

Antimicrobial agents usually are defined as something which has a negative effect on micro-organisms. Based on the antimicrobial strength, the antimicrobial effect can be divided into several categories: slowing the rate of microbial growth, stopping microbial growth, killing some percentages of microorganisms over time, killing percentages of germ quickly and killing all microorganisms including spore-formers within 10min. Depending on the strength of antimicrobial effect, the antimicrobial textiles could also be applied in different circumstances.

Many kinds of biocidal agents have been utilized to impart antimicrobial functions to polymers, such as N-halamine, antibiotics, chitosan, quaternary ammonium salts, phophonium compounds and metal salts (Kenawy, Worley & Broughton, 2007; Majumdar et al., 2009; Lee, Yeo & Jeong, 2003). However, usually their attachment to a textile surface or incorporation within the fiber substantially reduces their activity and limits their availability. Furthermore, the biocide can be gradually lost during the use and washing of the textile. For

these reasons, large amounts of these biocides need to be applied to textiles to effectively control bacterial growth and to sustain durability.

Many heavy metals are toxic to microbes at very low concentrations either in the free state or in compounds. They kill microbes by binding to intracellular proteins and inactivating them. The antimicrobial function of it is effective and durable (McDonnell & Russell, 1999). They could be blended into polymer before extrusion or in the electrospinning process.

Quaternary ammonium compounds (QAC), particularly those containing chains of 12–18 carbon atoms, have been widely used as disinfectants. These compounds carry a positive charge at the N atom in solution and inflict a variety of detrimental effects on microbes, including damage to cell membranes, denaturation of proteins and disruption of the cell structure (McDonnell et al., 1999). During inactivation of bacterial cells, the quaternary ammonium group remains intact and retains its antimicrobial ability as long as the compound is attached to textiles. The attachment of QAC to a textile substrate is believed to be predominantly by ionic interaction between the cationic QAC and anionic fiber surface (Kim & Sun, 2001; Son & Sun, 2003).

Chitosan is the deacetylated derivative of chitin, which is the main component of the shells of crustaceans such as shrimps, crabs and lobsters (Rinaudo, 2006). Large quantities of chitin are produced as a by-product of the seafood industry. Chitosan has been found to inhibit the growth of microbes in a large body of work. The antimicrobial mechanism is not clear but is generally accepted that the primary amine groups provide positive charges which interact

with negatively charged residues on the surface of microbes. Such interaction causes extensive changes in the cell surface and cell permeability, leading to leakage of intracellular substances. This antimicrobial ability, coupled with its non-toxicity, biodegradability and biocompatibility facilitates chitosan's applications in food science, agriculture, medicine, pharmaceuticals and textiles (Rinaudo, 2006; Lim &Hudson, 2003).

N-Halamines are compounds containing one or more nitrogen-halogen covalent bonds and they are normally formed by the chlorination or bromination of imide, amide, or amine groups. N-halamine compounds are broad-spectrum disinfectants that have been used in water treatment. An oxidative reaction of *N* -halamines contributes to the inactivation of microorganisms which consumes the halogens. Then the halogens can be recharged by another chlorination or bromination treatment (Worley & Williams, 1998; Sun, Chen, Worley & Sun, 2001; Sun, Xu, Bickert & Williams, 2001; Sun, 2001).

Based on the antimicrobial strength and their characteristics, the agents were applied under different circumstances. For example, metal salts as silver could kill the microorganisms efficiently but be depleted after a slow release process. Silver was widely used in wound dressing while the costs limited its application in the protective textiles such as surgical gowns. In addition, some concerns have been expressed about the development of bacterial resistance to silver and quaternary ammonium salts. To be used in protective clothes, the efficacy of chitosan is much lower compared to N-halamine. It could just inhibit the growth of microbes and the handle of the fabric, together with some other physical properties, will be adversely affected (Hsieh, Huang, Z. K., Huang, Z. Z., & Tseng, 2004). N-halamine kills

the microbes quickly and is favourable for its durability to washing and regenerability. It fits well with the objective to develop antimicrobial PET used as reusable protective clothes in healthcare facilities.

3.2.2 Antimicrobial mechanism of N-halamine

There are two antimicrobial mechanisms of N-halamine. It could effect as chlorine-releasing agents and work as intact N-halamine moieties.

They can be partially regarded as chlorine-releasing agents (CRAs), which exert the antimicrobial functions by releasing positive chlorine into the environment, and the positive chlorines react with appropriate receptors in the cells to achieve biocidal functions. Organic N-halamines can be classified into three types based on their chemical structures: imide N-halamines, amide N-halamines, and amine N-halamines. Due to the differences in the localized chemical environments, their stabilities follow the order of imide N-halamines < amide N-halamines < amine N-halamine, and their antimicrobial activities have a trend of imide N-halamines > amide N-halamines>amine N-halamine (Worley et al., 1988). We can find out the better stabilites, the worse antimicrobial activities. Surprisingly, despite being widely studied, the actual mechanism of action of CRAs is not fully known. CRAs are highly active oxidizing agents and thereby capable of destroying the cellular activity of proteins (Bloomfield, 1996). Increased penetration of outer cell layers may be achieved with CRAs in the unionized state. CRAs have deleterious effects on bacterial DNA that involve the formation of chlorinated derivatives of nucleotide bases (Dennis, Olivieri & Kruse, 1979; Shih & Lederberg, 1976). Because HClO with concentrations below 260 ppm does not

induce bacterial membrane disruption or extensive protein degradation, it was inferred that DNA synthesis was the sensitive target. CRAS have also been found to disrupt membrane-associated activity. Higher concentrations of CRAS are sporicidal and also possess virucidal activity (Bloomfield & Arthur, 1992; Best, Springthorpe & Sattar, 1994; Bloomfield, Smith-Burchnell & Dalgleish, 1990). The spore coat material and the spore cortex could be removed and degraded by the interaction with the hypochlorite ion (Kulikovsky, Pankratz, & Sadoff, 1975). The RNA in virus could be inactivated and degraded by chlorine (Taylor & Butler, 1982).

Besides the positive chlorine resulting from the dissociation of N-Cl bonds which might be partially or completely transferred to the appropriate acceptors in the cell leading to expiration of the organisms, there could be another action mechanisms responsible for the biocidal efficacies of the N-halamine based materials. The intact N-halamine moieties could also have biocidal effect, which might remain bound to cell membranes after partial penetration into the cells (Williams, Swango, Wilt & Worley, 1991; Williams, Elder & Worley, 1988). This action might also contribute to the observed inhibitory effect particularly if the quantity of free chlorines released to the wet environment was not sufficient enough to inactivate some tough species. Once inside or bind to the cell membrane, various enzymes or enzyme systems in the cell could be subjected to inactivation or inhibition.

3.2.3 Immobilization of N-halamines on fabrics

In the recent years, a lot of work has been done to immobilize the N-halamine to different polymers. Liu et al. successfully grafted some amide monomers such as acrylamide and methacrylamide to cotton cellulose. The products demonstrate durable and regenerable biocidal functions against Escherichia coli (Liu & Sun, 2006; Liu & Sun, 2009). The results also showed unproportionally low N-halamine contents with high graft yield which indicated nonnegligible side reactions during graft polymerization. Luo et al coated polymethacrylamide (PMMA) onto the surfaces of Kevlar fabrics by a in situ polymerization of methacrylamide with coating polymer binders. The synthesized fabric showed durable, and rechargeable biocidal activities against *E. coli* (gram-negative bacteria), *S. aureus* (gram-positive bacteria), *C. tropicalis* (fungi), MS2 virus, and *Bacillus subtilis* spores. They all demonstrated the antimicrobial ability of acyclic N-halamine treated polymer fibers (Liu & Sun, 2008). Poly(ethylene terephthalate) (PET) could also be made biocidal by incorporating acyclic N-halamine compounds. Liu et al. also grafted monomer 3-allyl-5, 5-dimethylhydantoin (ADMH) onto poly-(ethylene terephthalate) (PET) fabric and demonstrated that benzoyl peroxide could generate macromolecular radicals on PET when it was delivered to the areas properly. But it seemed that reaction occurred at the end or defect areas, thus little monomers can be grafted, and total kill of 10^5–10^6 CFU/mL Escherichia coli at a contact time of 2 h can be achieved which is not very effective (Joiner, 2001).

3.2.4 Evaluation of Antimicrobial Efficacy

A number of test methods have been developed to determine the efficacy of antimicrobial textiles (Aizenshtein, 2007). These methods generally fall into two categories: the agar

diffusion test and suspension test. The agar diffusion tests use AATCC 147-2004 (American Association of Textile Chemists and Colorists), JIS L 1902-2002(Japanese Industrial Standards) and SN 195920- 1992 (Swiss Norm). They are only qualitative, but are simple to perform and are most suitable when a large number of samples are to be screened for the presence of antimicrobial activity. Suspension Test includes AATCC 100-2004, JIS L 1902-2002 and SN 195924-1992. These methods provide quantitative values on the antimicrobial finishing, but are more time-consuming than agar diffusion tests. The bacterial species Staphylococcus aureus (Gram positive) and Klebsiella pneumonia (Gram negative) are recommended in most test methods. These two species are potentially pathogenic and therefore require proper physical containment facilities for handling.

Many studies have used the innocuous Escherichia coli (Gram negative) as a test microorganism which can be cultured and handled in a standard laboratory with minimal health risk.

3.3 PET

3.3.1 Application of PET in healthcare facilities

Several kinds of materials were widely used in hospitals including cotton for the clothing and towels, nylon-spandex blend for the pressure garments and polyvinyl for the splash aprons, polyester and cotton-polyester blend for the scrub suits, surgical gowns, lab coats and drapes, etc. Among those materials, because of its good mechanical properties, durability, thermal stability, ease of processing and low production cost, polyethylene terephthalate (PET) is a the most favoured candidate material to make reusable barrier protective textiles in hospitals.

Thousands of tons of waste are generated worldwide in hospitals each day. Depending on region and hospital, the weight percentage of textiles in medical waste ranges from 11% to 26%.(Diaz, Eggerth, Enkhtsetseg & Savag, 2008; Sabour, Mohamedifard & Kamalan, 2007; Hamoda, El-Tomi & Bahman, 2005; Altin, S., Altin, A., Elevli & Cerit, 2003) A good strategy to reduce waste is reuse. Textiles are among the materials in health-care settings which have reduction, recycling, and reuse potential. Accounting in the costs of waste disposing, initial purchase price and warehousing costs, the prices of per disposable product are twice as expensive as reusables and when they are laundered correctly reusable products performs 70% better protection than the latest disposable spun-bonded producs. Using disposable medical materials also generates a huge enviormental burden. As reusable medical textiles have received attention due to their advantage of reducing waste and cost and offering more efficient protection,(Aizenshtein, 2007) the production and consumption of reusable PET in medical application such as scrub suits, lab coats and privacy drapes increased continually in recent years. Between 2004-2008, the manufacture of PET fibers and yarn increased by 31% from 38 to 50 million tons. However, PET is susceptible to contamination of many microorganisms including bacteria, viruses and spores [3,4,5] and the contaminated PET can serve as one of major sources of infectious diseases. To decrease the possibility of cross-infection, it is necessary to introduce antibacterial property/function to PET surface. However modification of PET is challenging because of its chemically inert characteristics, high crystallinity and hydrophobicity.

3.3.2 PET surface modification

Many technologies have been attempted in the surface modification of PET fabrics. Blending, coating and grafting are the most commonly used methods to add new functionalities to PET surface.

3.3.2.1 Physical surface modification

Functional particles could be blended into polyester before extrusion and bring functions to polyester surface. Impregnation of polyester with cationic copper endows it with antimilcrobial functions. Impregnation of copper oxide was achieved by adding a cupric oxide powder to the polymer during the master batch preparation stage before extrusion. The treated fabric could kill $1*10^5$ CFU *S. Aureus* in 2 h and $4*10^6$ CFU *E.coli* in 1h. (Gabbay & Borkow, 2006)

3.3.2.2 Chemical surface modification

The chemical functional modification of polyester is a great challenge. Firstly, there is not active functional group on polyester surface. Secondly, the chemical nature of PET does not allow the formation of an appreciable quantity of radicals on macrochains.

At last, monomer diffusion on it is poor especially with long chain monomers for its high crystallinity and hydrophobicity (East, 2005). One approach is to coat the PET using compounds with functional group or other polymers. The compounds can be coated with interfacial chemical bonding. Cyclic N-halamine siloxanes has been coated to the PET surface through bond of hydroxyl and carboxyl fragments resulted by the hydrolyzation of

PET and siloxanes. The coated PET fabrics showed good biocidal properties in inactivation *staphylococcus aureus* and *Escherichia coli* and were stable under machine washing conditions. (Ren et al., 2008) But the hydrolysis reduced the tensile strength of the fibers and might impact the comfortability of textile. In addition, the amide monomers such as acrylamide and methacrylamide are more cheaper and commonly used. Oxygen plasma and wet chemical etching treatment can all prepare the surfaces of polyester substrates for bonding hybrid coatings rapidly (Aizenshtein, 2007). However, the coated polyester suffered from delamination and cracking of inorganic coatings when subjected to wet thermal cycling for the hydrolyzation of the binding bond. M. Rochery et al. locate copolymers siloxane–urethane onto polyester fabrics to make them hydrophobic (Gabbay & Borkow, 2006).

Silica impregnation is another efficient and attractive method to modify the surface of polyester substrates in which hybrid coatings can be incorporated by introducing an interlocking silica network within the polymer matrix. Silicon alkoxide incorporates into the polyester substrate forms a silica network what interpenetrated within the polyester structure. The network would extend to the surface of polyester. (Chou & Cao, 2003)

Radical graft polymerization is possibly the most powerful means for the chemical surface modifications of chemically inert polymers such as polyester. M. Louati et al. tried to graft Fluorine containing monomers to PET to improve water and oil repellency and chemical and thermal stability, etc (2007). However, even using a swelling liquid as a reaction medium, still little monomers can be grafted. Hydrophilic polyester were made relatively successfully by low frequency plasma polymerization of acrylic acid and treating with a mixture of He–Ar

gas plasma before grafted with acrylic acid (Song, 2006). Among these treatment methods for the surface modification of polymers, the photo-induced UV grafting onto polymer surfaces is a very interesting method for obtaining desired properties for specific uses, because it allows the surface characteristics to be altered without causing serious modifications to the polymer bulk mechanical properties and so is an attractive way to impart a variety of functional groups to a polymer. Y.-W. Song et al. irradiated the PET films coated with acrylic acid (AA) and altered the surface of the substrate (PET film) from hydrophobic to hydrophilic through this process, as confirmed by FT-IR, SPM and XPS analyses. However only little AA was added and it is possible that lots of them polymerized to PAA short chain (Deng et al., 2009). Researchers have also grafted ADMH onto PET fabric and rendered the treated fabric antimicrobial which was mentioned above. (Liu & Sun, 2008)

Up to date, several effective technologies have been applied to improve the surface properties of polymers. Compared with other modification methods, UV initiated surface grafting polymerization shows fast reaction rate and needs low cost of processing with simple equipment. Most importantly, the grafted chains are limited to a shallow region near the surface which offer the modification of surface properties without influencing the bulk material performance (Deng, Wang, Liu &Yang, 2009; Zhao & Brittain, 2000; Deng & Yang, 2009).

In UV induced graft polymerization, UV light is used to initiate surface graft polymerization, often in the presence of a photoinitiator. Compared with Norrish type I photoinitiators which leads to higher polymerization yield and rate, Norrish type II photoinitiators were more

widely used for its higher grafting efficiency (Deng, Yang & Rånby, 2000a). Benzophenone (BP) and its derivatives may are the most widely used type II photoinitiators (Decker & Zahouily, 1998; Pan, Viswanathan, Hoyle & Moore, 2004) shown to effectively initiate several surface photoiniated radical grafting polymerizations. In principle, BP or BP-based molecules are excited to a singlet state and then jump to a triplet state by intersystem crossing under UV irradiation. The triplet state molecule could perform hydrogen-abstracting reactions from substrates, and consequently provide surface radicals capable of initiating surface graft polymerization. The resulted benzopinacol radicals (BP–OH•) are less reactive and prone to take part in the termination reaction.

UV initiated grafting polymerization can be conducted in liquid phase (Chun et al, 1999), and the used solvents could have large influence on the grafting effects. Deng et al. (Deng, Yang & Rånby, 2000b) found that the grafting yield and the grafted chains distribution on surface could be greatly affected by the affinity of the solvent with the substrate, its absorption of UV light, and the reactivity and initiating ability of the solvent.

3.3.2.3 Thermoplastic semi-interpenetrating network

As mentioned above, many efforts have been directed to impart functional groups onto the chemically inert PET. The incorporation of functions into PET fibers has been accomplished by physical impregnation of functional particles before extrusion, coating on its surface with compounds with functional groups or functional polymers and surface radical grafting polymerization.

The formation of surface interpenetrating network (IPN) polymers could be used as a viable alternative to synthetic grafting techniques in upgrading the properties of chemically inert polymers like PET. (Liu, Zhao, Rudenja, 2009)Acrylamide (AM), divinyl crosslinker N,N'-methylenebisacrylamide (MBA) and photoinitiator benzophenone (BP) diffuse into the swollen surface of PET and polymerize in-situ to form a thermoplastic semi-IPN. It is named as such because the substrate thermoplastic PET is physically crosslinked, while the immobilized functional polymer is chemically crosslinked to physically interlock with the substrate polymer. Thermoplastic IPN involves only physical crosslinks (crystalline areas serve as crosslinking point); in semi-IPN, one linear or branched polymer is blended with another chemically crosslinked polymer network. Neither of the two definitions fits this situation so two descriptors “Thermoplastic“, “Semi“ are combined to reflect the similarity between the synthesis of this structure and the other two IPNs. The immobilized polyacrylamide (PAM) is durable upon Soxhlet extraction with distilled water for 72 hours, and also upon refluxing with methanol for 24 hours.

This technique possesses the advantages of limiting the modification to a shallow region on the PET surface without compromising the bulk properties, achievable high immobilizing efficiency/density, easy and mild reaction conditions, and versatility in introducing a variety of functional groups onto the surface of various semicrystalline polymer substrates.

3.4 Conclusions

Nosocomial infection and antibiotic resistance have become serious problems in recent years while contamination through textiles is one of the major sources. Polyester is widely used in

hospitals as nurse uniforms, surgical gowns and protective drapes, etc. Therefore it is critical to introduce antimicrobial function into polyester. Through immobilizing N-halamine into polyester we can get regenerable antimicrobial polyester. The formation of thermoplastic semi-IPN by in-situ photoinitiated polymerization could be a promising way to immobilize N-halamine precursors on polyester surface which is simple and clean, has little influence to the mechanical properties of the polymer, and could accomplish one side modification. The N-halamine based polyester was expected to have effective antimicrobial functions.

Chapter 4: Experiment Methods

4.1 Materials

Polyester woven fabric was purchased from Test Fabrics Inc. (West Pittiston, PA). Polypropylene (PP) woven fabric was purchased from----. Acrylamide (AM), benzophenone (BP), divinylbenzene (DVB), 2-ethyleneglycol diacrylate (EGDA), N,N'-Methylene bisacrylamide (MBA) and some other reagents were purchased from Aldrich. Azobisisobutyronitrile (AIBN) (TCI America, Portland, OR) was recrystallized from ethanol. Cross-linker DVB with 1000ppm 4-tert-butylcatechol was washed four times with an equal volume of an aqueous solution of 10% sodium hydroxide, followed by four rinses with deionized water, in order to remove the inhibitor. The monomers and polymers have been specified in Table 1.

Table 1 Monomers and Polymers

AM= Acrylamide, MAM= Methacrylamide BP = Benzophenone AIBN= Azobisisobutyronitrile DVB= mixture of divinylbenzene isomers MBA=N,N'-Methylene bisacrylamide EGDA=2-ethyleneglycol diacrylate	
PET= Poly(ethylene terephthalate), PAM=Polyacrylamide, PMAM= polymethacrylamide	
PAM-PET	PAM-PET-M = thermoplastic semi-IPN between PET and PAM, crosslinker: MBA PAM-PET-D = thermoplastic semi-IPN between PET and PAM, crosslinker: DVB PAM-PET-E = thermoplastic semi-IPN between PET and PAM, crosslinker: EGDA

4.2 Immobilization on fabric by photo-initiated polymerization

A novel surface modification technique was applied in our study. Polyamide was immobilized onto fabrics by forming an interpenetrating network (IPN). Amide monomers, divinyl crosslinkers and photoinitiators diffuse into the swollen surface of PET and polymerize in-situ to form a thermoplastic semi-IPN. UV irradiation was adopted here to initiate the polymerization since it is desirable to limit the immobilized polyamide chains to a shallow region near the surface.

PET fabrics were surface-modified with polyamide by forming an interpenetrating network on substrate surface. Briefly, a PET fabric swatch with a diameter of 4.25 inch was firstly swollen in methanol solution of initiator, monomer, and crosslinkers. In the research, usually two swelling conditions were adopted to achieve the immobilization percentage (IP) of modified PET fabric as 13%: swelling at 20 ^{o}C at standstill for 7 days and at 40^{o}C shaking at 90rpm in the shaking bath for 30 min. In the study of effect of swelling duration (1-7 days), irradiation duration (15-60min) and different initiators, the first swelling condition were used while in the further study to save time the second swelling condition was used. Different components were tried in the modification, such as different monomers AM and MAM, different initiators BP and AIBN, and different crosslinkers MBA, DVB and EGDA. The swell and immersion process of PP fabric presented at 40^{o}C in the same way in butanol solution for 2h. Excess solution was dripped off from the specimen and absorbed by the filter paper for 5s to achieve around 120% sorption of the solution. The PET and PP fabric were then exposed to UV irradiation (365 nm) for 60 min and 120 min respectively. After the polymerization, the sample was extracted with distilled (DI) water in a Soxhlet-extractor for

24 h, dried at 105^{o}C, and stored in a desiccators (humidity<20%) for 48 h to reach constant weight.

The immobilization percentage was calculated from the following equation:

$$\text{Immobilization percentage (IP)} = (W_2 - W_1)/W_1 * 100 \quad (1)$$

where W_1 andW_2 are the weights of the pristine and the modified PET samples, respectively.

4.3 Characterization

4.3.1 FTIR and elemental analysis

FTIR spectra were taken on a Nicolet 380 spectrometer (Thermo Electron Corporation) using KBr pellets.

Carbon, Hydrogen & Nitrogen contents on PET samples were examined following elemental analysis at the Guelph Chemical Laboratories Ltd.

4.3.2 X-ray Photoelectron Spectroscopy

All XPS data were acquired with a Kartos Axis Ultra spectrometer by Kratos Analytical, Inc. This instrument unitlizes a monochromatized Al KR X-ray source, a hemispherical analyzer for spectra acquisition, a concentric mirror analyzer for chemical imaging, a multichannel Delayed Line Detector (DLD), and a low-energy electron flood gun for charge neutralization. The X-ray spot size used for these experiments was approximately 700 μm × 300 μm in size for spectra collection, and 400 μm × 400 μm spot for imaging with Field of View 2 (FOV2) lens configuration deployed. The vacuum in the analytical chamber during spectral acquisition was better than 1×10^{-9} Torr. For elemental composition determination, survey

spectra were acquired at analyzer pass energy of 160 eV. The high-resolution of all individual elements spectra were acquired at an analyzer pass energy of 40 eV. The takeoff angle (the angle between the sample normal and the input axis of the energy analyzer) was 0 ° if not noted otherwise. This takeoff angle corresponds to a sampling depth of approximately 55 A. One or two spots on one or two replicates were analyzed for each sample treatment.

The Vision 2 software by Kratos Analytical was used to determine peak areas, calculate the elemental compositions from those peak areas, and peak fit the high-resolution spectra. Carbon, oxygen, and nitrogen concentrations were calculated from the C1s, O1s, and N1s lines in 0-1100 eV survey scans. The binding energy scale was calibrated by assigning the hydrocarbon peak in the C1s high-resolution spectra to a binding energy of 284.7 eV for pristine PET and polyacrylamide (PAM) immobilized PET. A Gaussian-Lorenzian line shape was used to peakfit the high-resolution spectra, with a Shirley background subtraction.

4.3.3 Iodometric titration

An iodometric titration method was adopted in quantification of the active chlorine content on the samples. 0.26 g to 0.27 g of sample fabric was cut into small pieces and then added into 25 mL of 0.001 N sodium thiosulfate standard solutions. After 30 min shaking, the excess amount of sodium thiosulfate in the mixture was titrated with 0.001 N iodine standard solutions by monitoring mV changes with a redox electrode (platinum Ag/AgCl). The active chlorine concentration of the modified PET samples was then calculated from the following equation:

$$\text{Active chlorine concentration } [Cl^+] \text{ (ppm)} = 35.45 \times (V_1 - V_2) \times N \times 1000 / (2 \times W) \quad (2)$$

where V_1 and V_2 are the volumes (mL) of the iodine solution consumed in titrations of blank sodium thiosulfate solution and that with PET sample in, respectively, N is the normality of iodine solution and W is the weight of the samples in grams. Conversion ratio of N-H to N-Cl can be calculated from the following equation:

$$\text{Conversion ratio (\%)} = [\text{Cl}] \times M(\text{AM})/(\text{IP} \times M(\text{Cl}) \times 100) \quad (3)$$

where M(AM) and M(Cl) are the molecular weight of the acrylamide and chlorine respectively.

4.3.4 Titration of surface COOH groups

About 0.2g of PET samples were immersed into 10ml ethanol solution of thionine acetate (A_1, V_1) (0.5 mg/ml) and the reaction solution was stirred at room temperature for 10 h. The sample was taken out, washed four times with ethanol and all solutions were combined (A_2, V_2) UV adsorption of which was then recorded (wavelength = 605 nm, ε = 54300). The amount of carboxylic acid groups on unit weight of PET sample can be calculated according to the following equation:

$$[\text{COOH}] = (A_1 \times V_1 - A_2 \times V_2) / (\varepsilon * b * W) \quad (4)$$

where A_1 and A_2 are the UV absorptions of the original thionine acetate solution and the combined solution after test, V_1 and V_2 are the volume of the original thionine acetate solution (10 ml) and the combined solution after test, b is the path length (1cm), and W is the weight of the tested PET sample.

4.3.5 Swelling ratio test

Before the test, PET samples were stored in desiccators for 48 h to reach constant weight (W2).Then 0.2 g of the equilibrated PET sample was immersed in 100 ml of distilled water. After 1 h, the sample was separated from the contacting solution and placed in a centrifuge tube with the bottom half filled with cotton fiber to retain the spin off solution. The centrifuge was carried out at 1200 rev/min for 15 min. The weight was recorded immediately after the centrifugation (W1). The weight was recorded immediately after the centrifugation (W1). The swelling ratio is expressed as the ratio between the weight of the wet sample and that of the dry sample, i.e.,W1/W2. The swelling ratio of immobilized PAM network could be calculated from the ratio of PAM-PET and PET pristine.

$$\text{Swelling ratio of immobilized PAM} = (W1/W2 \times (1+IP)-W0'/W0)/\ IP \quad (5)$$

where W_0' and W_0 are the weight of the wet pristine PET and dry pristine PET respectively, and IP is the immobilization percentage of the studied PAM-PET fabric.

4.3.6 Swelling kinetics study

The kinetics of the swelling process was investigated by means of the weight test at 20 ℃. Samples are weighed on an electronic balance (precision 0.001 g), and then kept immersed in water. The samples were taken out of the liquid at specific time (set as 0 min, 2 min, 4 min, 10 min, 30 min, 1 h, 2 h), the water adhering to the surface was removed by centrifugation for 4 s, and the samples were weighed. The time for each weighing was kept to a minimum (at most 1 min). This procedure continues till equilibrium swelling was achieved.

The mol percent uptake Qt, [%mol/g] is defined as

$$Q_t = ((m_1-m_0)*M/m_0)*100 \quad (6)$$

where m_t is the weight of swollen sample after time interval t, [g]; m_o is the initial weight of dry sample, [g]; M is the molecular weight of water,18 [g/mol].

To show the responsive dimensional change of the PAM-PET yarn, optical microscopy was used. To make a sharp edge visible, the iodine solution (0.01N) was used as immersion solution. A piece of fabric ($1*1cm^2$) was laid on a glass slide under objective glass. After 10 µl iodine solution dropped on the fabric, pictures was taken after 2, 4 and 10min.

4.4 Regenerability study

To assess the regenerability, the sample was treated with "chlorination-quench-regeneration" cycles. To form N-halamine structures on the modified samples, we bleached the modified PET fabrics by immersing them in sodium hypochlorite solution (1500 ppm available chlorine) at room temperature for 30 min. The liquid to fabric (liquor) ratio was 30:1 (w/w). The fabrics were then rinsed thoroughly with an excess amount of distilled water and air-dried for 24h. Then active chlorine content on the samples was investigated by iodometric titration. The active chlorine was quenched in the titration process which means the N-Cl was changed back to the N-H. The N-halamine structure could be regenerated from amide with another chlorination process.

4.5 Antibacterial Assessment

Antibacterial properties of the modified PET samples were examined according to a modified American Association of Textile Chemist and Colorists (AATCC) test method 100-2004 against several clinical important bacteria: healthcare-associated methicilin-resistant *Staphylococcus aureus* (HA-MRSA) isolate #70527, CA MRSA community associated methicilin-resistant *Staphylococcus aureus* (CA-MRSA) isolate #40065, *Staphylococcus*

aureus isolate ATCC# 25923 , multidrug resistant extended spectrum *beta - lactamase* (MDR ESBL) isolate #70094 and multidrug-resistant *Pseudomonas aeruginosa* (MDR P. Aeruginosa) (obtained from the CANWARD study assessing antimicrobial resistance in Canadian hospitals, www.canr.ca). The fabrics were cut into two small pieces (4.8 cm in diameter), and one piece of fabrics was put in a sterilized container. 100 μL of an aqueous suspension containing10^5–10^6 colony forming units (CFU)/mL of the bacterium was placed onto the surface of the fabric. Then the inoculum on the fabric was then covered with another piece of same fabric. To ensure sufficient contact, a sterilized 100ml beaker was place onto the top of the fabrics. After various contact times, the inoculated samples were placed into 10 mL of 1.0% sodium thiosulfate aqueous solution to neutralize any active chlorine. The mixture then went through vigorously shaking for 2 min and ultrasonic treatment for 5 min. An aliquot of the solution was removed from the mixture and then serially diluted and 100 μL of each dilution was placed onto a nutrient agar plate. The same procedure was applied to both the bleached unmodified and modified but unbleached PET fabrics as controls. Viable bacterial colonies on the agar plates were counted after incubation at 37 ℃ for 18 h. Bacterial reduction is reported according to the following equation

$$\text{Percentage reduction of bacteria (\%)} = (A - B)/A \times 100 \quad (7)$$

where *A* is the number of bacteria counted from the control fabric, and *B* is the number of bacteria counted from modified fabric.

The bottom piece of fabric was also further investigated by leaving it on an agar and culturing for 48 h at 37 ℃. Before placement of the fabric on the agar, the fabric also contacted the agar 5 times at different parts pressed by a sterile 100 ml beaker.

4.6 Moisture Diffusion test

Type 684 Automated Water Vapour Diffusion Apparatus was employed to evaluate diffusion and transportation of moisture through fabrics. This apparatus was designed and built by S.E.A. Engineering Company and was used to measure the rate at which water vapor diffuses through fabrics. The test was performed according to Canadian Standard CAN/CGSB – 4.2 No. 49-99. Four circular test specimens, with a diameter of 4.25 inch (10.795 cm), were cut from each sample in such a way that i) no two specimens contained the same warp or weft yarns (in case of woven materials), and ii) no specimen was taken from creased or damaged area of the sample. All specimen samples were conditioned in accordance with CAN/CGSB-No. 2. It means all specimens were conditioned in a standard testing atmosphere of 65 $\pm$ 2 percent relative humidity and 20 $\pm$ 2 degree Celsius for at least 24 hours prior to testing. There were 6 intervals runs for each sample: two blank runs before and after the 4 runs with specimens.

The following calculations were performed using this testing standard.

1- For each specimen tested, the slope was calculated using mass and time to determine the water vapour transmitted per second Mx (kg/s).

2- Average mass of water vapour transmitted per unit time M (kg/s) was determined from the four individual determinations of Mx (kg/s).

3- The vapour resistance (R) of a square meter area of the sandwich was calculated using the relation:

$$R = A \Delta P/M \quad (8)$$

Where:

A = the area of the specimen exposed to the water vapour, in square meters. ΔP = the difference in partial pressure of water vapour across the sandwich in Pa. This is equal to the saturation vapour pressure. M = the average mass of water vapour transmitted per unit time, in kg/s.

4- The vapour resistance of the empty cell R_B was calculated using the above equation and the data from the blank runs.

5- The vapour resistance of a unit area of the material Rm was calculated in m ₱a.s/kg using:

$$Rm = R - R_B \quad (9)$$

6- This value of R was converted to units of millimeters of equivalent still air, Dm by dividing by Rair. Rair is the resistance of one millimeter of still air at 20 ° C and one atmosphere of pressure.

$$Dm = Rm / Rair \quad (10)$$

Where: The resistance of one millimeter of still air at 20 °C and one atmosphere

of pressure is $5.4x10^6$ m^2 Pa s/kg. For other conditions of temperature and

pressure it varies as:

$$Rair = 5.4 \times 10^6 (Pa / 101.3) (Ta / 293)$$

Where: Pa = Atmospheric Pressure [kPa], Ta = Air temperature [₹K]

4.7 Air permeability test

Air permeability is an important factor in the performance of textile materials. It can also be used to provide an indication of the porosity and/or breathability of weather-resistant and rainproof fabrics. Construction factors and finishing techniques can have an effect upon the air permeability by causing a change in the length of airflow paths through a fabric.

In this study, the low pressure Frazier Air Permeability Instrument was used. This test measures the air permeability in terms of the number of cubic feet of air passing through one square foot of fabric per min when the differential air pressure between opposite sides of the fabric is equal to 0.5 inch of water. It is applicable to all types of fabrics and to a variety of other permeable materials in sheet form. A circle of fabric was clamped (circular test head had a test area of 4.25 square inches) in the testing device, taking care to smooth out any wrinkles or creases before clamping. The air pressure differential was adjusted to 0.5 inch water gauge pressure. This differential was measured by means of an inclined oil or water manometer with a slope of 1:10. The volume of air passing through the specimen was measured by means of a calibrated orifice. The pressure change at the orifice was observed with a suitable manometer. Three specimens were test for each kinds of sample.

4.8 Statistical analysis

In the study, antibacterial tests (Figure 19) are performed in duplicate, and other measurements are conducted in triplicate except research of influence of crosslinker concentration on the IP (Figure 9) and swelling kinetics (Figure 14). The results are expressed as means ± standard deviations.

Chapter 5: Results & Discussions

Several semicrystalline thermoplastic polymers such as PET and PP are widely used in medical applications including non-biodegradable sutures, extracorporeal mechanical lung, surgical gowns and protective clothing, etc. They are favoured for their mechanical property, durability and resistance to biological degradation. However, some new functions as durable antimicrobial function on the surface of surgical drapes to decrease the possibility of cross-infection in hospitals are often necessary to fulfill certain application requirements. Surface modification is difficult for chemically inert polymers. We developed a new method in immobilizing functional polymers onto the surface of chemically inert semicrystalline thermoplastic polymeric substrates. It is proposed to polymerize functional monomer and crosslinker in the swollen surfaces of the polymers to form interlocking structure and durably immobilize the functional groups on their surfaces. The fabrics were modified by forming a thermoplastic semi-IPN. (Scheme 1) In-situ photo-polymerization under UV following diffusion of amide monomers, crosslinkers and photoinitiators into the surface of polymer substrate which was swollen in mutual solvent resulted in the stable entrapment of the polyamides.

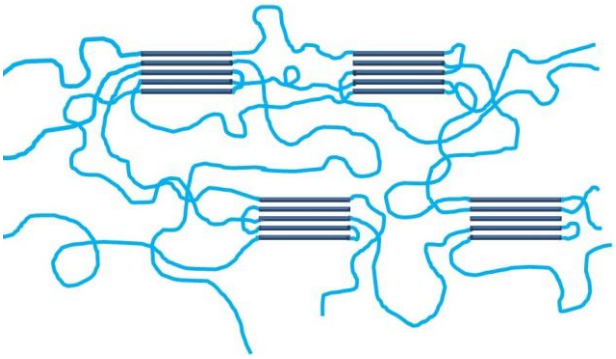

Swelling of the
semicrystalline
polymer network

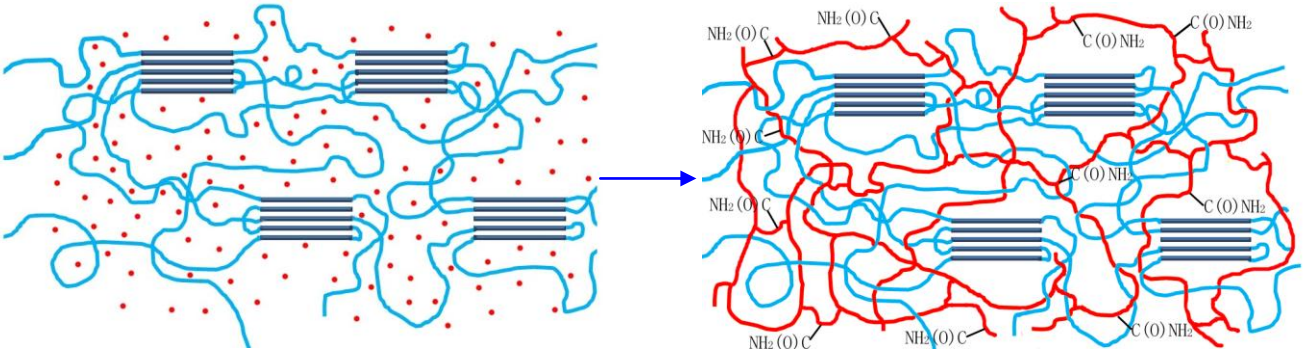

Penetration of monomer

and crosslinker into the network

In-situ polymerization:

interpenetration network

Scheme 1 Formation of thermoplastic semi-interpenetration network

Red dots represent monomer acylamide (AM) or methacrylamide (MAM) and crosslinker N,N'-methylenebisacrylamide (MBA);
Red lines represent crosslinked poly(acrylamide) or poly(methacrylamide)

5.1 Immobilization of polyamides on PET

Two vinyl amide monomers (AM and MAM) were immobilized onto polyester by forming thermoplastic semi-IPN of polyamide through a UV induced polymerization. PET fabric was soaked in methanol solution of monomer AM or MAM, crosslinker BAM and initiator BP

for 7 days. The excess solution on fabric was dripped off and then the fabric was irradiated under 365nm UV for 1h. Under UV, photoinitiator benzonphenone (BP) molecules are excited to a triplet state and undergo hydrogen-abstracting reactions with solvent methanol and generate methoxy radical which initiate co-polymerization of BAM and AM/MAM. The adoption of UV initiated polymerization could limit the reaction to surface and decrease the possible negative impact on the bulk properties of PET substrates.

After graft polymerization, all the treated fabrics went through 24h soxhlet extraction. Water was used as extraction solvent to remove the unreacted monomers and loosely attached polymers.

5.1.1 Durability of the immobilization

The modified PET fabrics were challenged with Soxhlet extraction with distilled (DI) water for 24h, 48h and 72h to test their durability.

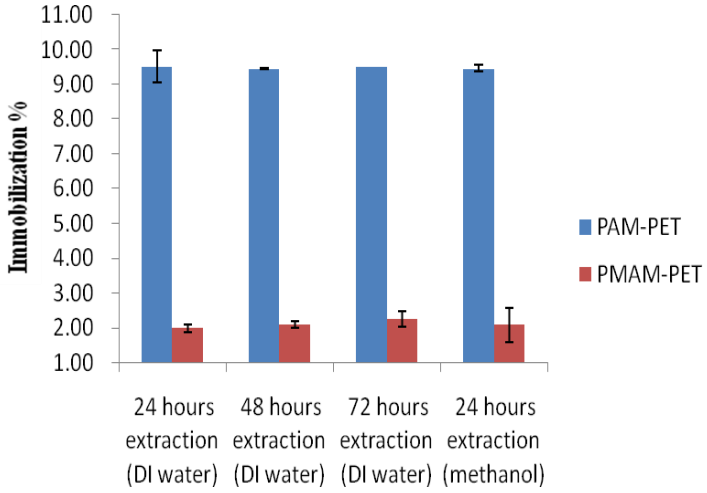

Figure 1 Effect of Soxhlet extraction on the immobilization percentage

* AM/MAM 2 mol/l, MBA 0.045 mol/l, BP 0.055 mol/l

As water is a good solvent for polyamides, the unstably attached polymers could be removed by the extraction. Immobilization percentage (IP) stayed consistent after 24h to 72h extraction. (Figure 1) The immobilized PAM and PMAM are also stable against 24 hours methanol extraction following the 72 hours DI water extraction which can allow further derivatizations of the immobilized functional groups. Such results showed the good durability of the modified fabrics. As 24h extraction is sufficient to remove immobilization which is not durable so it is set as routine for further study.

The IP of PAM-PET is much higher than that of PMAM-PET with the same recipe. This is due to both the more efficient formation and more successful immobilization of acrylamide. The polymer radical reactivity is inversely proportional to the Q values of the monomers as reported by Otsu (Decker, 1989). The Q values of AM and MAM are 1.2 and 1.46 respectively. So the reactivity of AM radical is higher than MAM radical. Resulted by the low radical reactivity of MAM and steric hinderence of its monomer, the propagation rate of AM should be quicker. Then the formation of PAM network could be quicker. On the other hand, the crosslinker MBA would work less efficiently with MAM. MBA even has a higher reactivity ratio than AM and can form longer sequence in the copolymerization. Formation of longer sequences behaving as multi-functional knots could significantly decrease the crosslinker efficiency. This problem is more serious when the MBA is comonomer, so its network could not immobilize on substrate as much as PAM network. Hence the below discussion will focus on PAM-PET system

5.1.2 Confirmation of the immobilization by forming IPN

To further confirm the expected immobilizations, PAM-PET was characterized by FTIR spectroscopy. Figure 2 shows spectrum (a), a FTIR spectrum of polyacrylamide (PAM) modified PET (PAM-PET), spectrum (b), a FTIR spectrum of pristine PET, and spectrum (c), result of subtracting FTIR spectrum of pristine PET from that of PAM-PET. The subtraction spectrum between pristine PET from that of PAM-PET fits well with that of PAM. The successful immobilization of PAM on PET is confirmed by the peaks at 3422 and 3193 cm^{-1} which are attributed to the symmetric and asymmetric stretching of N-H in $–C(O)NH_2$ and characteristic amide I and II peaks of PAM locating at 1660 and 1609cm^{-1}.

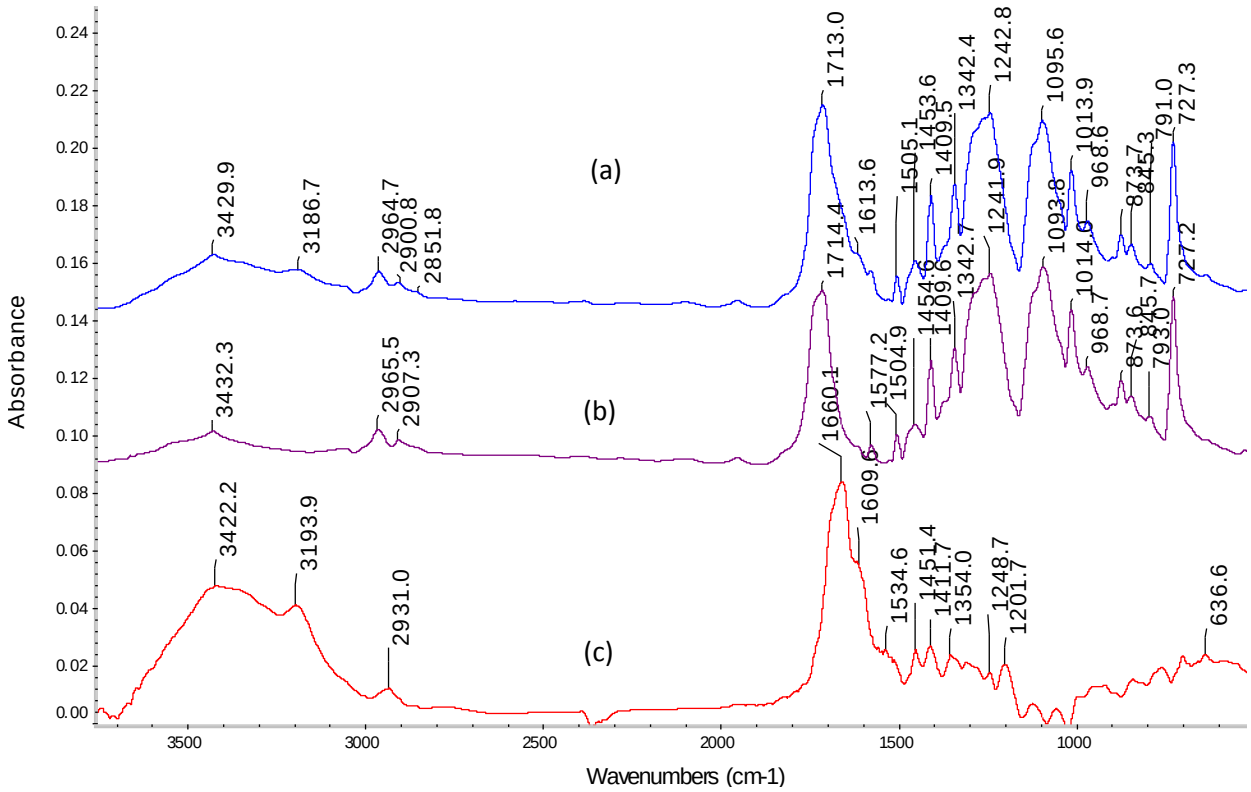

Figure 2 FTIR spectra of (a) polyacrylamide (PAM) modified PET (PAM-PET); (b) pristine PET; (c) subtracted FTIR spectrum of PAM-PET and pristine PET.

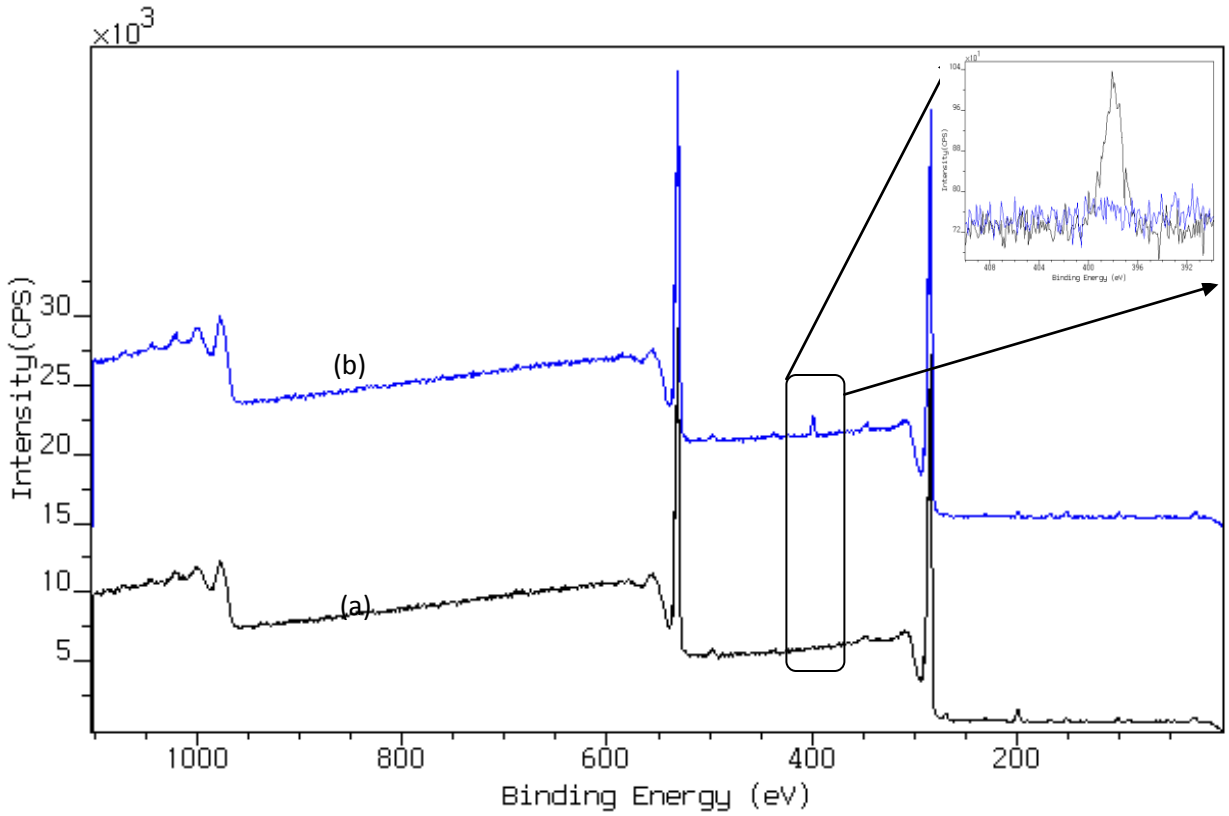

Figure 3 XPS Survey of (a) pristine PET and (b) PAM-PET (immobilization percentage 15.5%)

The successful immobilization of PAM on PET is also evidenced by existence of N element in XPS spectra of PAM-PET in Figure 3. There is no detectable nitrogen in pristine PET whereas a clear nitrogen peak shows up in PAM-PET at 400 ev.

The immobilization of PAM in the form of interpenetrating network was proved by the further study of the modified fabric by Modulated-Temperature Differential Scanning Calorimetry (MTDSC) accomplished by Dr. Song Liu. Because of the frozen impact of the IPN on the mobility of PET, its Tg varied. His study also showed that the IPN can be destroyed by melting which further confirmed the formation of IPN.

The immobilization percentage (IP) of polymer on PET will significantly influence the surface properties of the modified fabric. For example, the variation of IP of PAM-PET will

change its swelling properties, surface morphology and its efficiency of antibacterial function. In the novel modification method, the IP could be controlled by adjusting the components, concentrations and parameters in the polymerization. These rules obtained in this study could also be applied in the study of versatile functional modification with the method.

5.1.3 The immobilization mechanism

As a Norrish type II photoinitiator benzophenone could perform a hydrogen abstraction reaction with the substrate. So it was chosen as an initiator in this study. PAM could be immobilized to PET in two ways: grafting of PAM chain on PET backbone and immobilization with crosslinker as a network. Because under the solvent condition, BP may abstract hydrogen majorly from methanol instead of from PET substrate, the major mechanism of immobilization may still be the formation of the interpenetrating network: thermoplastic semi-IPN. So another initiator AIBN which is known as a poor initiator in grafting polymerization was also adopted in the reaction. Data are listed in Table 2. The results show that there is no significant difference between the IP of PAM-PET with these two initiators. So the immobilization should majorly attributed to the formation of network.

Table 2 Immobilization percentage of PAM-PET vs. different initiators

Immobilization Percentage (%)	Initiator	
	BP	AIBN
PAM-PET 1[a]	13±2	12±3
PAM-PET 2	21±3	25±3

a. Recipe for PAM-PET 1: AM 3.0 mol/l, MBA 0.045 mol/l, initiator 0.055 mol/l; Recipe for PAM-PET 2: AM 5.0 mol/l, MBA 0.045 mol/l, initiator 0.055 mol/l;

As the antibacterial performance of PAM-PET could be significantly affected by its IP, the effects of a few parameters in the immobilization process on IP were studied such as irradiation duration, swelling duration, crosslinker types and crosslinker concentration. By adjusting these variables, the IP on PAM-PET could be controlled.

5.1.4 Effect of irradiation duration on the immobilization

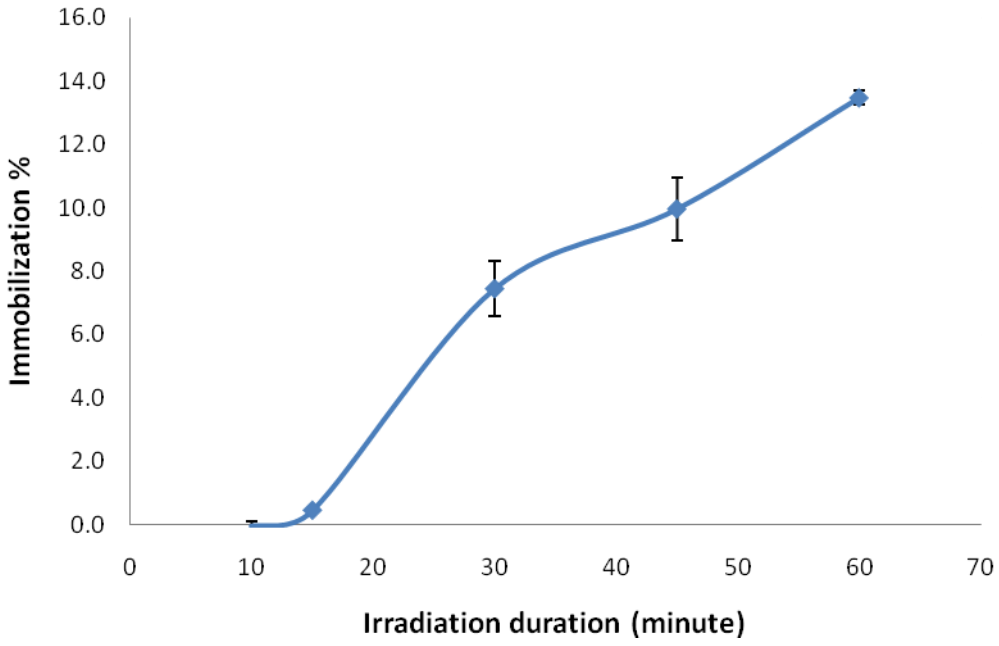

.

Figure 4 Effect of irradiation duration on the immobilization percentage of PAM-PET

* AM 3 mol/l, MBA 0.045 mol/l, BP 0.055 mol/l

Figure 4 represents plot of the immobilization percentage as a function of the irradiation time. More PAM could be immobilized on PET substrates as irradiation duration increases.

The UV light turning on and oxygen inhibition of radical polymerization deferred the activating of the immobilization. The oxygen dissolved in the solution, as well as the atmospheric O_2 diffusing into the sample during the UV exposure would scavenge the free

radicals formed by the photolysis of the initiator (Gnanou, 2008). This caused the very slow immobilization rate at first.

In the subsequent stage of immobilization, the plot showed increasing of slope which indicated the acceleration in the rate of immobilization. This was due to gel effect in the polymerization. The evaporation of methanol which caused increased viscosity leads to a significant reduction of termination rate. Because concentration of radicals is established by balancing rates of initiation and termination, a drop in the latter rate increases the concentration of radicals and accelerates propagation(Gnanou, 2008).The steady increase of grafting percentage in the period also proved the effective immobilization of PAM molecule chains assisted by crosslinker.

After 35min, the slope of the immobilization decreased. This would due to two reasons. Firstly, because of huge loss of methanol, the viscosity of solution increased greatly, which led to the difficulty of monomer diffusion. Thus, the kinetic rate constant values would decrease as polymerization proceeds. Secondly, for the higher reactivity of MBA indicates lower and lower molar fraction of crosslinker in residual comonomers as polymerization proceeds which could cause more unsuccessful immobilization of many homopolymerized PAM molecule chains compared to last two stages. It fits well with the three stages in the crosslinking copolymerization of AM/BAM: pre-gel reactions, gelation and postgel reactions (Zhong, Ishifune & Yamashita, 2000)

The sorption of the finishing solution after 7 days soaking was about 3.1 g in which the total weight of monomer, initiator and crosslinker was 0.698 g. The saturated grafting percentage

is 60.5% while the grafting percentage with 1 h irradiation is only 13.5% which indicate only small part of the compounds was immobilized. This could majorly due to the evaporation of solvent which hindered the polymerization and the partially unsuccessful immobilization of PAM oligomer.

5.1.5 Effect of duration of swelling on the immobilization

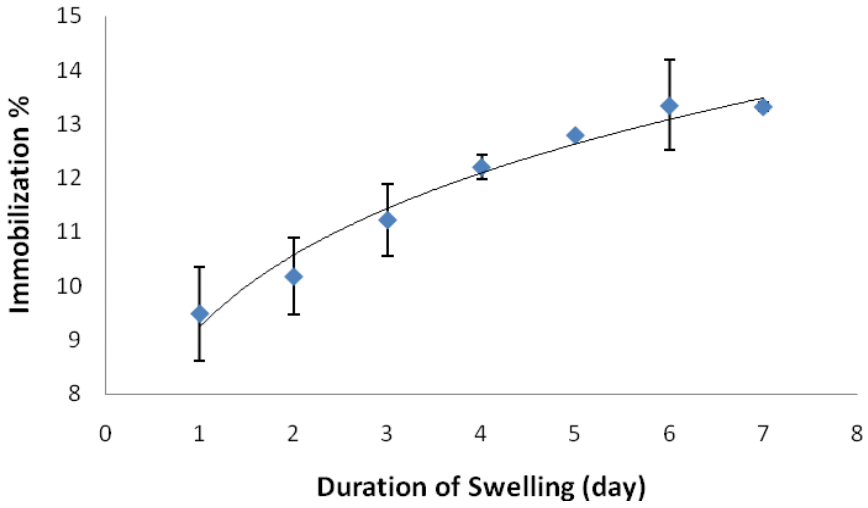

Figure 5 Effect of duration of swelling on the immobilization percentage of PAM-PET

* AM 3 mol/l, MBA 0.045 mol/l, BP 0.055 mol/l

Figure 5 shows the effect of duration of swelling on the immobilization percentage It takes time for the penetrant transportion of methanol and diffusion of monomers in semicrystalline PET. With longer swelling time, more monomers could be up-taken and take part in the polymerization. So the immobilization percentage increased with the swelling time. It was reported that the methanol transport in the thermally crystallized PET versus the square root of the swelling time $t^{1/2}$ should give a linear line. (Zhong, Ishifune & Yamashita, 2000) Actually, the result in Figure 6 showed that a straight line fits well with the immobilization

percentage plot vs. $t^{1/2}$ (Figure 7, R^2=0.98). It indicates that the amount of the immobilized polymer is proportional to the uptake of methanol solution.

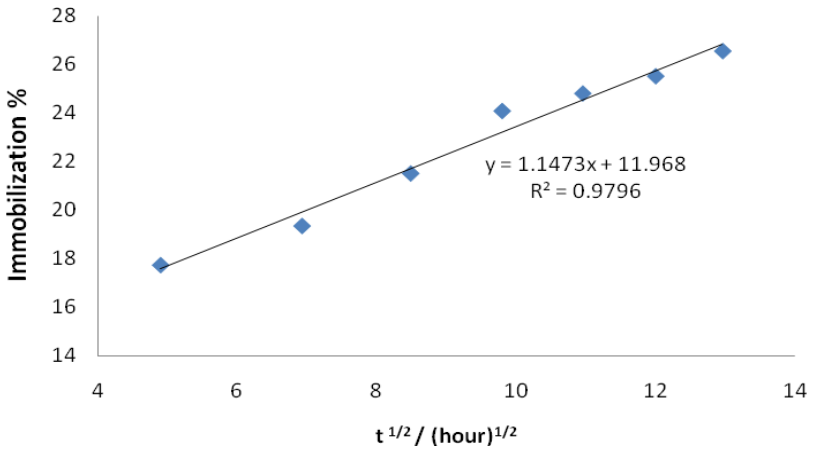

Figure 6 Immobilization percentage of PAM-PET versus the square root of the swelling duration $t^{1/2}$

5.1.6 Effect of monomer concentration on the immobilization

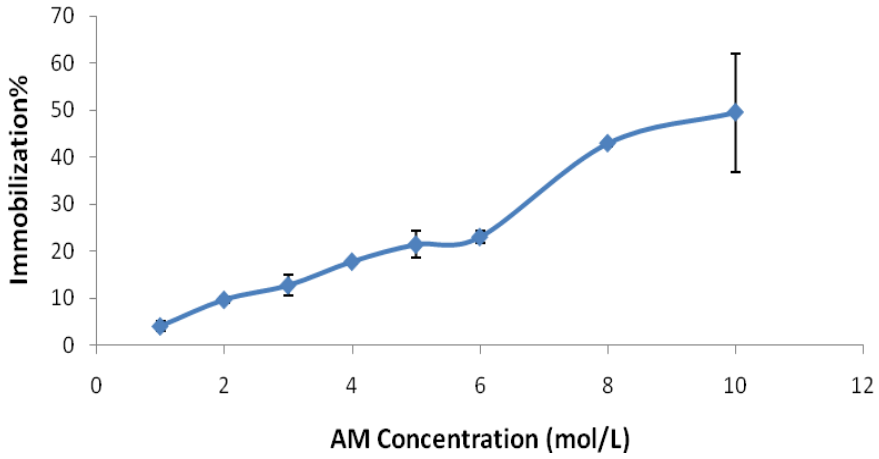

Figure 7 Effect of monomer concentration on the immobilization percentage of PAM-PET

* AM 3 mol/l, MBA 0.045 mol/l, BP 0.055 mol/l; irradiation: 60 minutes

As shown in Figure 7, immobilization percentage of PAM increases with the monomer concentration. As the monomer concentration increases, relative ratios of monomer to both

initiator and crosslinker increase which will result in longer kinetic chain length and quicker polymerization. At the same time, as the crosslinker has a high tendency to react with itself to form higher sequence hence causes lower efficiency in network formation. So increased monomer to crosslinker ratio can decrease the effect and increase the crosslinker efficiency. For these two reasons, the increase of the monomer concentration could contribute to the more efficient and better formation of the interpenetrating network. In addition, the linear tendency offers us the potential to easily control the IP of the modified fabric based on monomer concentration. Once the monomer concentration reaches 10 mol/l, the immobilization is obviously not uniform and cause tension among the fabric, which is why the variation of the immobilization percentage is bigger than other points.

5.1.7 Effect of crosslinkers types on the immobilization

Vinyl monomer AM was co-polymerized respectively with MBA, DVB and EGDA (structure of which are shown in Scheme 2) in methanol swollen PET to form a thermoplastic semi-IPN. PET fabric was soaked in methanol solution of monomer AM, crosslinker (MBA, DVB or EGDA) and photo-initiator benzophenone (BP) at 40^{o}C for 30 min and then the excess solution was allowed to drip off and then absorbed with filter paper for 5s before exposing the fabric to 365 nm UV irradiation. The swelling conditions are intensified to decrease the swelling duration of PET and penetration of the monomers into the fabric. After 1 hour irradiation, the modified PET fabric was Soxhlet extracted by DI water for 24 h to remove un-reacted monomers and unattached polymers. The swelling conditions are adjusted to achieve the same IP with the previous 7 day condition based on the same recipe. The surface morphology of the modified fabrics also shows the same appearance with the previous study.

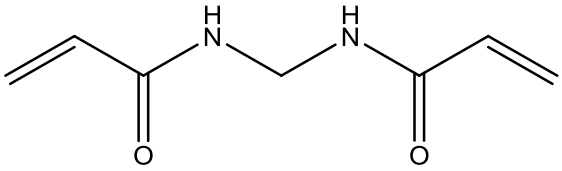

MBA

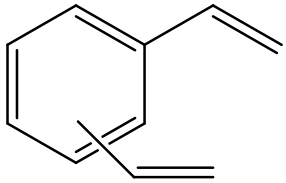

DVB

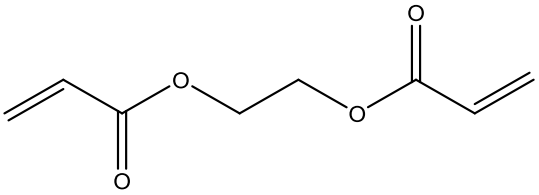

EGDA

Scheme 2 Structure of the three crosslinkers (MBA, DVB and EGDA)

With all the three crosslinkers MBA, DVB and EGDA, PAM could be efficiently immobilized on PET surface by forming the thermoplastic semi-IPN confirmed the FTIR spectra (Figure 8). All the modifided PET fabrics are specified in Table 1.

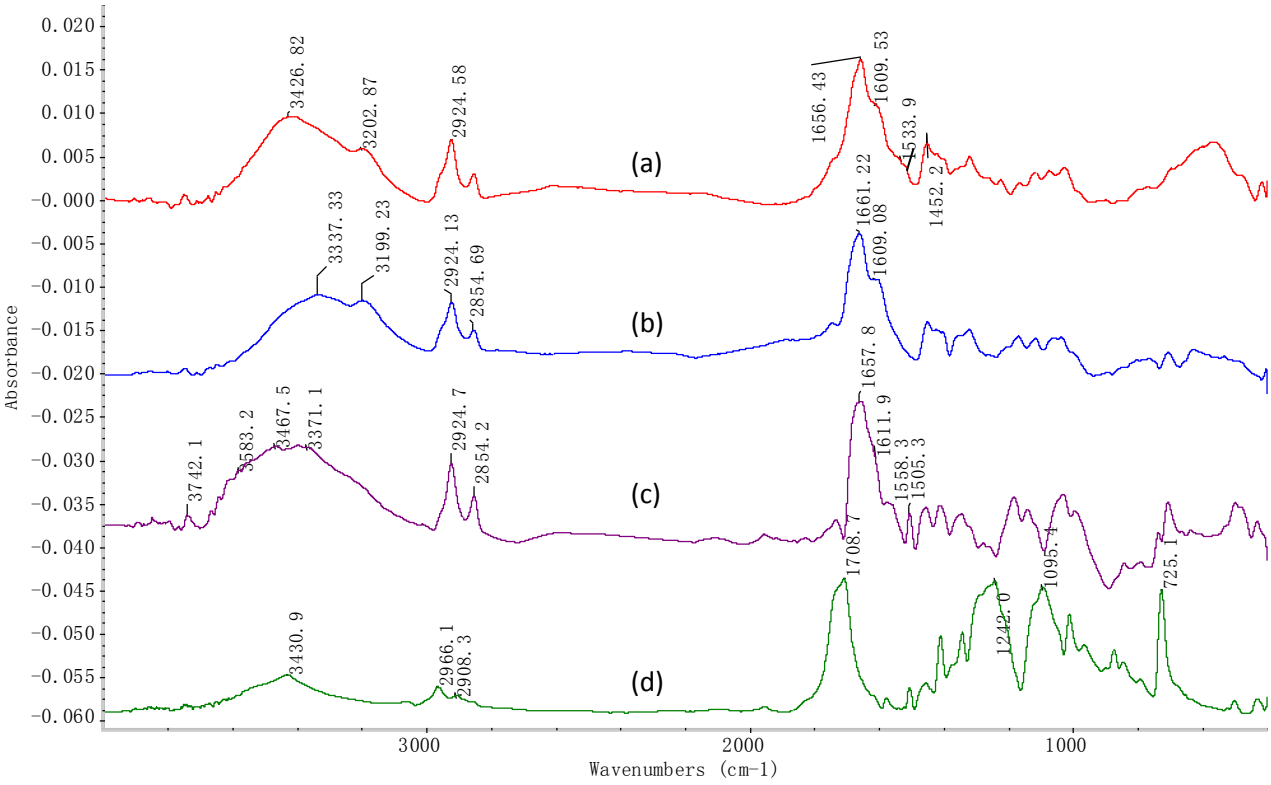

Figure 8 Subtracted FTIR spectra between a) PAM-PET-M and pristine PET, b) PAM-PET-D and pristine PET, PAM-PET-E and pristine PET and d) FTIR spectra of PET pristine

Figure 8 shows four FTIR spectra. Spectrum (a) is a result of subtracting the FTIR spectrum of pristine PET from that of PAM-PET-M (thermoplastic semi-IPN between PET and PAM, crosslinker: MBA); spectrum (b) is a subtracted FTIR spectrum between PAM-PET-D (thermoplastic semi-IPN between PET and PAM, crosslinker: DVB) and pristine PET; spectrum (c) is the subtracted FTIR spectrum between PAM-PET-E (thermoplastic semi-IPN between PET and PAM, crosslinker: EGDA) and pristine PET. All three spectra show the characteristic amide I peak of PAM in the range of 1656 to 1661 cm^{-1}. Spectra a) and b) show peaks at 3427/3337 cm^{-1} and 3203/3199 cm^{-1} corresponding to symmetric and asymmetric stretching of N-H in $-C(O)NH_2$. Characteristic amide I and II peaks of PAM locate at 1656/1661 cm^{-1} and 1609 cm^{-1} respectively. Compared to spectrum b), the red shift of N-H stretching from 3337 cm^{-1} to 3427 cm^{-1} and the additional medium peak at 1534 cm^{-1}

on spectra a) are due to the –NH-CO- structure of the immobilized crosslinker MBA in PAM-PET-M. Because of the high hygroscopicity of PAM-PET-E, even after long term drying there was still trace amount of water in the sample. The broad peak from 3100 cm^{-1} to 3600 cm^{-1} originating from water obscures that of amide peaks in the region.

Table 3 The immobilization percentages and active chlorine concentration of the modified PET fabrics

Sample	Immobilization percentage (IP)	[Cl][a]	Conversion ratio
	%	ppm	%
PAM-PET-M	13.9	1373	1.98
PAM-PET-D	5.8	1047	3.61
PAM-PET-E	6.2	794	2.56

*AM concentration 3mol/l and crosslinker/monomer ratio 1.5%, BP 0.055 mol /L
a) Available chlorine 1500ppm, bleached for 20 min

As shown in Table 3, the immobilization percentages of PAM-PET-D and PAM-PET-E are much lower than that of PAM-PET-M. This is majorly due to the different reactivity ratios of DVB, EGDA and MBA in copolymerization with AM. In copolymerization, the reactivity ratios r_1 and r_2 of two comonomers are defined as: $r_1=k_{11}/k_{12}$ and $r_2=k_{22}/k_{21}$, where kij is the rate constant of the reaction between growing polymer chain with monomer i unit readical and monomer j. As reported by Baselga, (Baselga, Llorente, Hernandez-Fuentes & Pierola, 1989) in the chain crosslinking copolymerization of AM and MBA in water, the reactivity ratio of them are 0.57 and 3.36 respectively. Although the reactivity ratios of AM and DVB (or AM and EGDA) have not been reported yet, we could predict the network buildup system through similar studies done by other researchers. It was found out that the reactivity ratios of AM and styrene in ethanol are 0.30 and 1.44. (Billovits & Durning, 1988) The reactivity ratios of trifunctional crosslinker trimethylolpropane triacrylate and acrylic acid in radical polymerization were reported as 0.77 and 3.6, respectively. Then we can predict that in the

copolymerization of AM and DVB, the reactivity of DVB is much higher than AM and AM radical prefers to react with DVB. As reported, the propagation rate constant of AM and styrene are 15.8×10^{3} $L.mol^{-1}.s^{-1}$ and 145 $L.mol^{-1}.s^{-1}$ respectively. (Pascal & Winnik, 1993; Barner-Kowollik, Vana & Davis , 2002) The reactivity of syrene radical is significantly smaller than AM radical. Because of the high reactivity of DVB monomer, it tend to participate in the polymerization and conversed to a quite stable radical which will retard the polymerization of AM. As a result, the polymerization of AM could be hindered by DVB and the number of successful interlocked polymer chains in PAM-PET-D is dramatically smaller than that in PAM-PET-M during the given reaction time (1 hour). This would be the major reason for the smller IP of PAM-PET-D. In addition, the segmental diffusion could also influence the network formation in the copolymerization. The polymerization of EGDA and AM could show similar phenomenon with MBA and AM considering the similar reactivity ratios. In the previous study of copolymerization of AM with crosslinkers EGDA or MBA, it is reported that the crosslink density of the formed hydrogel is different even starting with the same monomer and crosslinker concentrations. The hydrogel crosslinked with EGDA has lower crosslinking density and shows higher swelling capacity. (Caykara & Turan, 2006) Lower crosslinking desnity of PAM-co-PEGDA system generates in less successfully interlocked polymer chains, leading to lower immobilization percentage (IP).

5.1.8 Effect of the crosslinker concentration on immobilization

The concentration of the crosslinker has significant influence on the immobilization. Becuase the structures of MBA and EGDA are quite similar, the reactivity ratio of them would be similar, results in similar influence of the concentration on the IP as shown in Figure 9. In the

first stage, the higher crosslinker concentration is, the more AM is immobilized and the bigger IP is achieved. Along with increased crosslinker concentration, more polymer chain interlocks could be formed within PET substrate, hence IP of PAM increases. When the crosslinker concentration is higher than 10 mol% of monomer, the IP drops as shown in Figure 9. That means the efficiency of crosslinker decreased dramatically. Because MBA has a higher reactivity ratio than AM, when the concentration of MBA is high they will effect as monomers and can form long sequence by themselves. Longer sequences behave as multi-functional knots with crosslinking efficiency progressively smaller with respect to isolated MBA. Simultaneously, both the steric hinderence and the difficulty of the diffusion of the crosslinker knot in the network exaggerated the efficiency decrease of the long MBA sequence. This resulted in the unsuccessful immobilization of MBA chains and the low IP. The second reason is increase of the time needed for the polymerization. At the same time, less efficiency of the crosslinker which caused the unsuccessful network formation would slow down the increasing of the solution viscosity, and then as result, it would take longer time for the radical copolymerization to get the gel point when the polymerization rate increases abruptly. So the total conversion ratio of monomer could decrease greatly in the limited 1h irradiation. Then less monomers could be immobilized and the IP drops. The third reason is the intramolecular cyclization which is a frequently happened side reaction in crosslinking polymerization at high crosslinker levels. It will form unreactive sites and speed up the termination of the polymerization. However, some cycles formed in this way still could be useful in the immobilization of the PAM on PET. The similar process happened with PAM-PET-E.

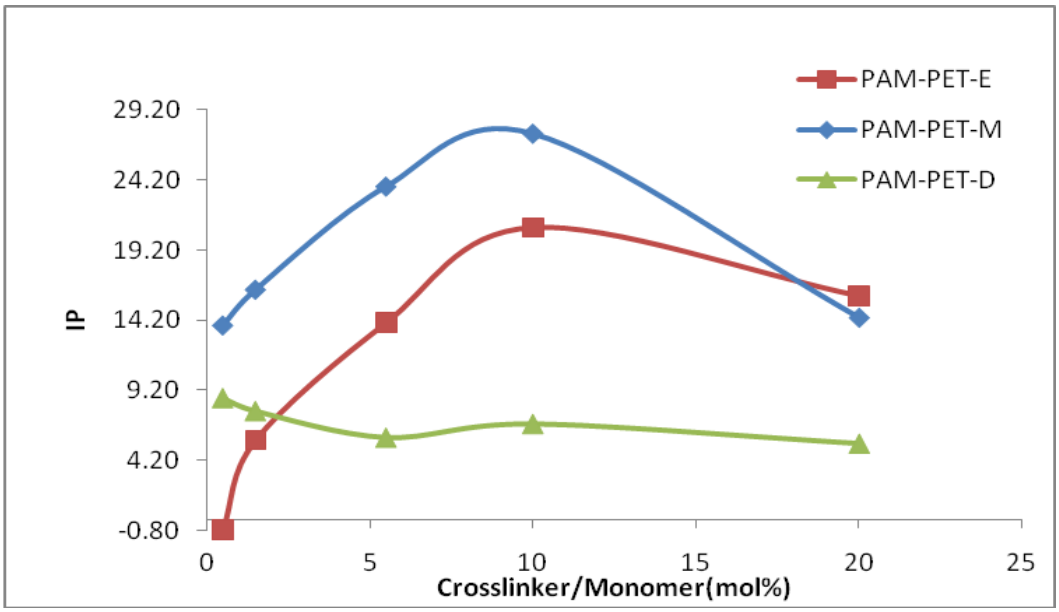

Figure 9 The influence of crosslinker concentration to the IP of PAM modified PET (AM 3 mol/L, BP 0.055 mol /L)

In Figure 9, the IP curve of PAM-PET-D is distinct from that of the other two samples. As discussed previously, in the copolymerization of AM and DVB, DVB could hinder the polymerization of AM, so the IP of PAM-PET-D is lower than the other two and the peak IP value on the curve of PAM-PET-D occurs in smaller crosslinker concentration as compared with the other two. In addition, for the high reactivity of DVB, its convertion could be higher than other two crosslinker, then the intramolecular cyclization has higher possibility to occur. As a result, when the DVB/AM molar ratio is smaller than 5%, the IP decrease with the increase of crosslinker concentration. As the crosslinker concentration keeps increasing, although the immobilized PAM decreased, the IP based on weight stayed consistent. This is due to the high convertion of DVB. At high crosslinker levels, it is highly possible that block segment of poly(divinylbezene) is formed and immobilized on PET. The big discrepancy between the IP of PAM-PET-D 20 (crosslinker/monomer ratio= 20%) samples based on nitrogen analysis and that based on weight gain is shown in Table 4. It indicates the immobilization of significant amout of poly(divinylbezene) contributes to the weight

increase after the modification. The PAM-PET-D 20 sample even after 24h extraction with water and 48h extraction with methanol showed a light yellow color which is similar to the color of pure DVB. This confirmed the existence of poly(divinylbenzene) on PAM-PET-D 20 sample. It was also found that the IP of PAM-PET-D can be raised to bigger than 9% by increasing AM concentration.

Table 4 The comparison between the IP calculated from N content and weight of PAM-PET-D with different crosslinker concentration

Molar ratio[a] %	IP (N) %	IP(W) %	S[b]
0.5	8.87	8.67	0.14
1.5	7.39	7.74	0.25
5.5	6.4	5.84	0.94
10	6.69	6.82	0.09
20	1.82	5.41	2.54

*AM concentration 3 mol/l and BP 0.055 mol /L,
a) Crosslinker/monomer molar ratio percentage(mol%); b)The standard deviation of the IP from N content IP(N) and weight IP(W) which shows the discrepancy between these two

5.2 Surface Characterization

As the immobilization of polyamide on PET is successful and controllable, efficient and controllable antibacterial performance could be expected. Protective PET is designed specifically to protect professionals such as healthcare workers and first responders. Currently, the widely used protective clothing is made of barrier textile materials that can block penetration and permeation of chemical solutions or human fluids through the fabrics. However, the barrier properties of the protective clothing also strongly affect the transport of heat and moisture generated by wearers, resulting in heat stress and low work efficiency. So besides antibacterial properties, the morphology and permeability change is also a major concern in the study

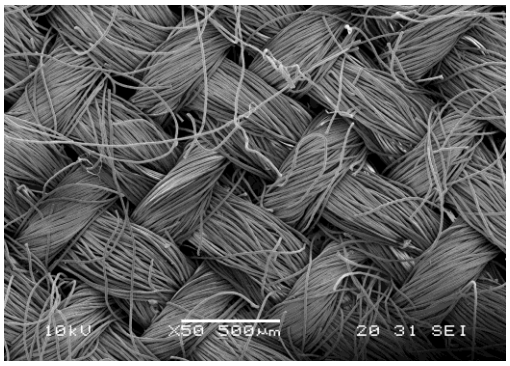

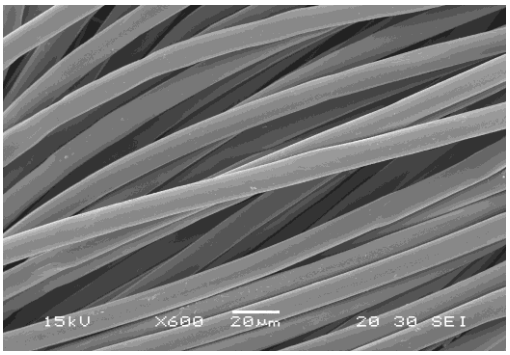

(a) Pristine PET

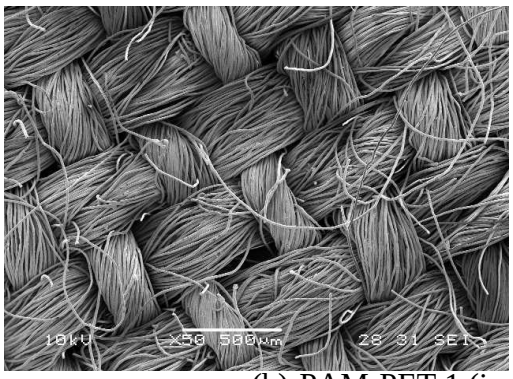

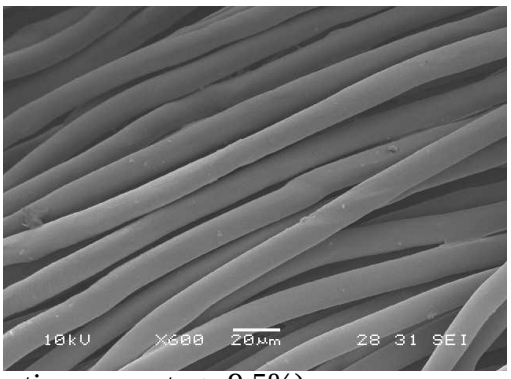

(b) PAM-PET 1 (immobilization percentage 9.5%)

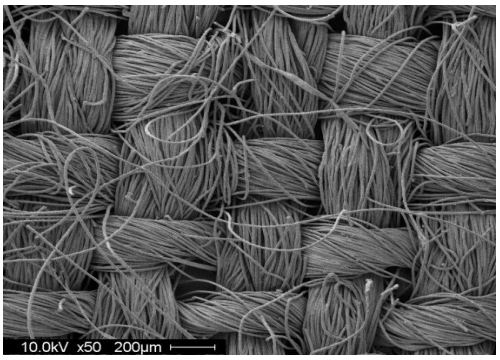

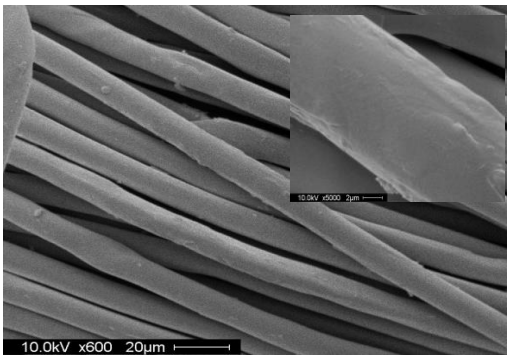

(c) PAM-PET 2 (immobilization percentage 13%)

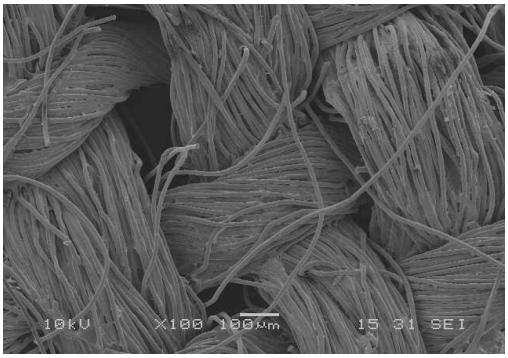

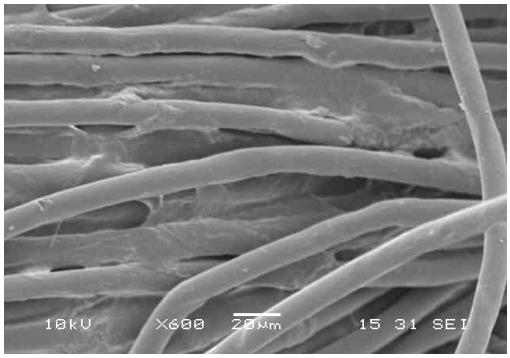

(d) PAM-PET 3 (immobilization percentage 21%)

Figure 10 SEM of PAM-PET fabrics

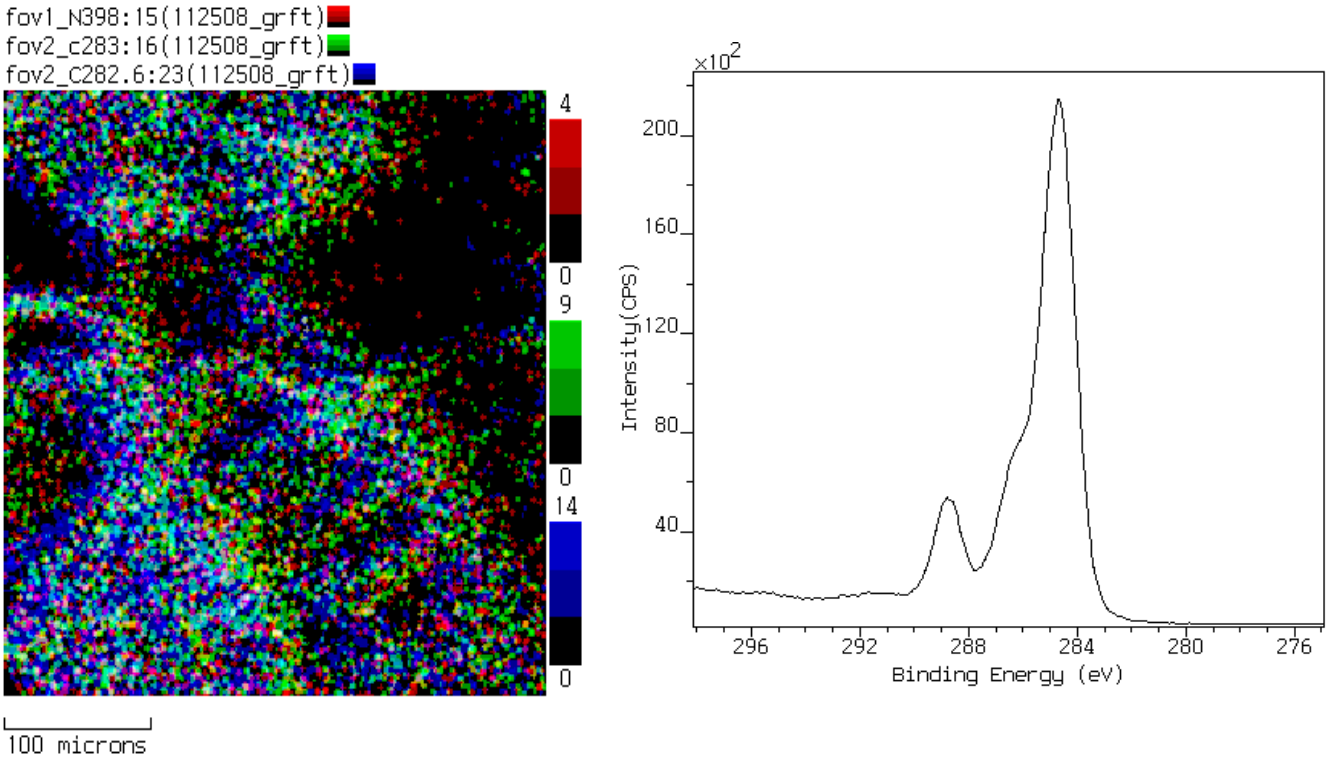

(a) (b)

Figure 11 XPS image (a) and high resolution C 1s XPS spectra (b) of PAM-PET (Immobilization percentage 9.5%)

As shown in SEM results (Figure 10), there is not obvious morphology change of the fabric under SEM until the immobilization percentage exceeds 20%. Even though there is no observable change of surface morphology for PAM-PET 1 (immobilization percentage 9.5%) under SEM, it can be seen that nitrogen is uniformly distributed along the yarns of the woven fabric in the element distribution map (Figure 11). The high-resolution of carbon spectrum (Figure 9b) shows three carbon peaks fitting well with the structure of PET. Once the IP is as big as 21%, the immobilization is obviously not uniform and cause tension among the fabric. Serious surface coating could be observable and interspaces between fibers are blocked. When the IP of the samples is as big as 13%, we can see clearly morphology change on the

fiber surface while the interspaces between the fibers and yarns are not blocked at all. Then the air and vapor transportation of the modified fabrics with IP less than 14% should not be significantly different with pristine fabrics.

5.3 Vapor permeability and air permeability

Finishing techniques can have an effect upon the air permeability by causing a change in the length of airflow paths through a fabric. Unchanged permeability ensures the possible comfort of the fabric after modification. To investigate the breathability of the modified fabrics, vapour and air permeability of the fabrics was studied. Diffusion and transportation of moisture through fabrics were studied according to Canadian Standard CAN/CGSB – 4.2 No. 49-99.

Table 5 The vapor permeability of the PAM-PET fabric (immobilization percentage 13%)

Sample	Thickness (mm)	Diffusion resistance of sample Dm (mm still air)
PAM-PET 2	0.48 ± 0.02	0.23 ± 0.27
Pristine	0.34 ± 0.01	0.21 ± 0.05

Because of the fire, vapour permeability study of the PAM-PET 1 and PAM-PET 2 could not be accomplished.

Two sample t-test was employed to evaluate the statistical significance of the results and a $p<0.05$ level of significance was used. As shown in Table 5, although the thickness of the PAM-PET 2 (IP=13%) increased significantly after the modification, its vapour permeability keeps almost the same. This could be explained by the observation in SEM test. Because

there is only slight surface morphology change on fiber surface and the interspaces between fibers keeps open. In fact, as the modification can increase the hydrophilicity of one side of the PET fabric, the vapour permeability performance could even possibly increase after modification when the vapour moves from the hydrophobic side to the hydrophilic side.

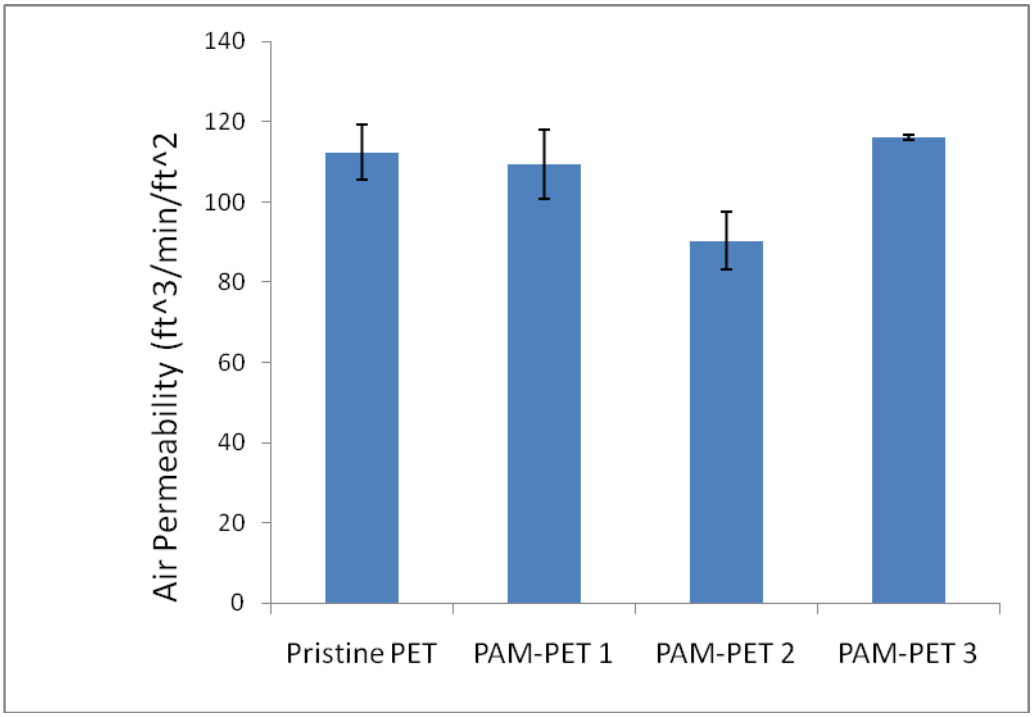

Figure 12 Air permeability of the PAM-PET fabrics

Air permeability is another important factor in the performance of textile materials. It can also be used to provide an indication of the porosity and breathability of fabrics. In this study, the low pressure Frazier Air Permeability Instrument was used. This test measures the air permeability in terms of the number of cubic feet of air passing through one square foot of fabric per min when the differential air pressure between opposite sides of the fabric is equal to 0.5 inch of water.

As we can see from Figure 12, the air permeability decreased as IP increase in the range from 0 to 13%. The difference between pristine and PAM-PET1(IP=9.5%) samples is not obvious when the air permeability decreased for less than 20% after 13% PAM immobilized on its surface by forming IPN. This is reasonable as considered the change in the SEM image. The decrease could also be attributed to the thickness increase after modification which will also increase the length of airflow path. Contrarily the air permeability of the PAM-PET 3 (IP=21%) fabrics is bigger than PAM-PET 2 (IP=13%) and even almost as big as pristine PET fabric. This could be due to the tension between the fibres caused by the connected surface coating which could decrease the "diameter" of the yarns and increased the interspaces between yarns in the end. As at the moment it is hard for the air to penetrate through the space in yarns, the broader space between yarns which is the major pathway for the airflow can cause the bigger air permeability.

5.4 Chlorination and Antibacterial performance

The self-disinfection function of the antibacterial PET could decrease the cross-infection in the healthcare facilities, so it is a major objective to achieve the effective antibacterial function after the modification. The amide immobilized on samples could be converted to N-halamine structures which is capable of quickly inactivating bacteria in a simple chlorination process: immersing the samples in a diluted chlorine bleach solution (1500 ppm available chlorine) at room temperature for 30 min. The liquid to fabric (liquor) ratio was 30:1 (w/w). The fabrics were then rinsed in distilled water and stored in a conditioning room (20 ℃, 65% relative humidity) for 24h. The active chlorine on the treated polyester is influenced by the concentration of available chlorine. Figure 13 shows the active chlorine achieved on the PAM-PET as a function of the available chlorine during the chlorination. Conversion ratio of

N-H to N-Cl increases with increased available chlorine concentration. Conversion ratios of amide to N-halamine were less than15% in the chlorination process of PAM-PET. This result is possibly due to (a) partially hydrolyses of the amide group, (b) less accessibility of the secondary amide hydrogen atoms due to steric hindrance, (c) ionic repulsion between chloro amine anion $CONCl^-$ and chlorinating agent ClO^- , (d) hydrophobic nature of the PET backbone which restricts the accessibility of chlorinating agents. Usually the amide groups on the surface of the fibers are mostly accessible to chlorine and can be converted to N-halamine structures.The higher chlorination concentration facilitates conversion of N-H to N-Cl. Once the available chlorine concentration exceeds 500ppm, the slope decreases. The slope change indicates the hindrance of additional chlorination which could be due to steric hindrance, ionic repulsion and lower accessibility of the secondary hydrogen on the amide groups. 20 min is enough to achieve the active chlorine saturation with certain chlorination concentration and IP. (Figure 13(b)) The result also shows that the active chlorine concentration on polyester could be adjusted either by the chlorination duration or the available chlorine concentration during the chlorination.

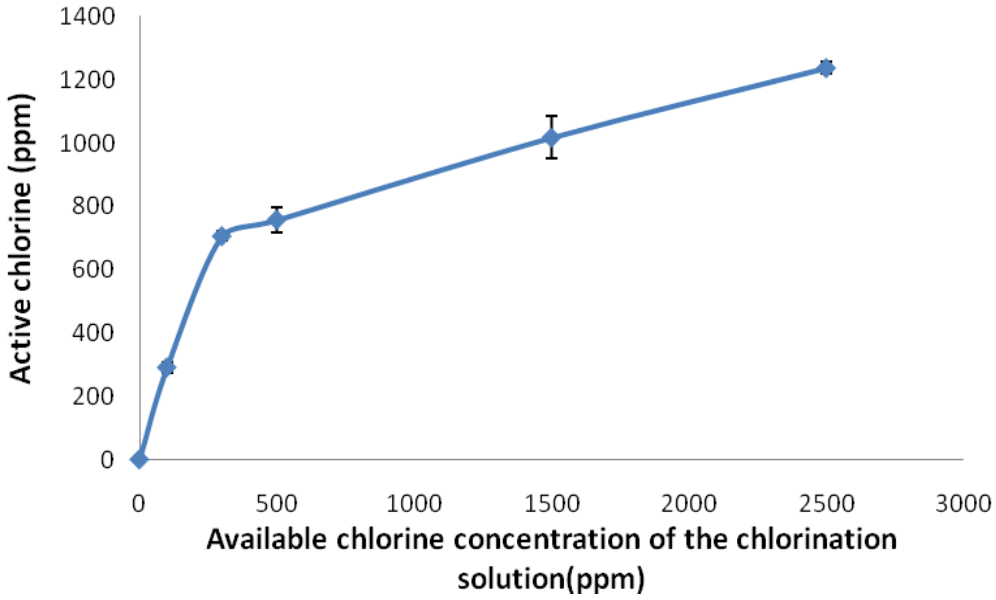

(a) Note: Chlorination duration is 30 min

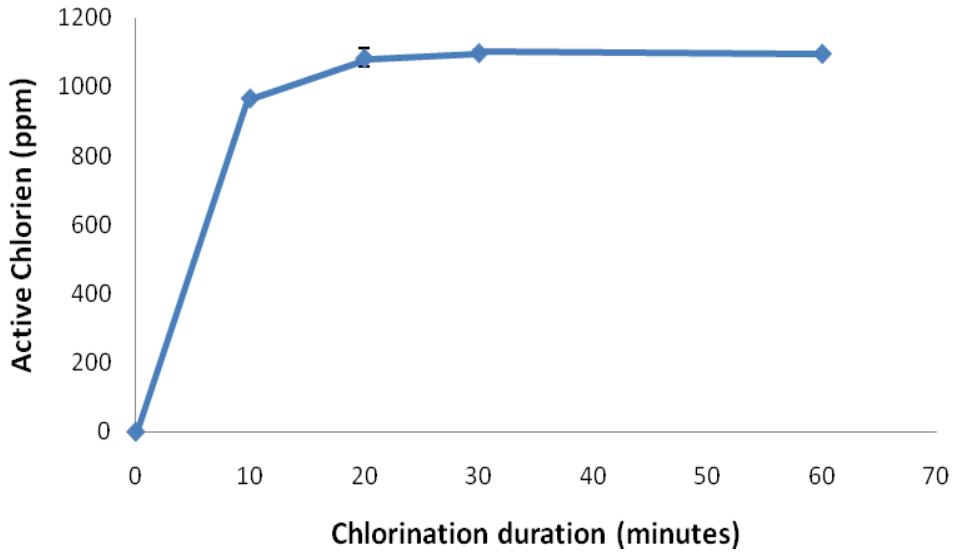

(b) Note: Available chlorine during chlorination is 1,500ppm

Figure 13 Active chlorine achieved on PAM-PET as a function of (a) the available chlorine concentration of the chlorination solution and (b) chlorination duration

The chlorinated PAM-PET samples were tested against 5 kinds of clinical significant bacteria *CA-MRSA* 40065, *HA-MRSA* 70527, *S.Aureus* ATCC 25923, *MDR ESBL* 70094 and

MDR P. Aeruginosa following the modified AATCC test method 100-2004. Table 6 shows the antibacterial efficacy of PAM-PET and PMAM-PET fabrics. At the active chlorine level of 1403 ppm, the PET fabrics demonstrated effective and rapid antibacterial property. HA-MRSA could be completely inactivated in 10 min. When active chlorine contents were in a range of 1141-1410 ppm, all the bacteria could be killed in 15 min. As the active chlorine on the fabric decrease, the total kill of all the HA-MRSA 70527 needs longer contact time (10min to 15min). Due to the low immobilization percentage of PMAM-PET (1.98%), the active chlorine on PMAM-PET is only 483 ppm so that the antibacterial performance is not as good as PAM-PET. However chlorinated PMAM-PET can still provide a total kill of 10^5-10^6 CFU/ml HA-MRSA in contact time of 30 minutes. The results prove that the active chlorine in N-halamine is the effective antimicrobial agent on treated fabrics. With N-halamine we can get effective antibacterial polyester used as durable protective textile in hospitals and some other health care facilities.

Table 6 Antibacterial efficacy of PAM and PMAM modified PET fabrics with different bacteria and active chlorine contents

				Reduction of HA-MRSA 70527 at different contact times %		
Grafted PET	Immobilization%	Chlorine	Bacteria	10 min	15 min	30 min
PAM-PET	13.2	1403±30	other 4	>90	100	100
			HA-MRSA 70527	100	100	100
		1158±17		96	100	100
PMAM-PET	1.1	483±20		82	-	100

*Other 4: *CA-MRSA* 40065, *S.Aureus* ATCC 25923, *MDR ESBL* 70094 and *MDR P. Aeruginosa*

5.5 Swelling properties

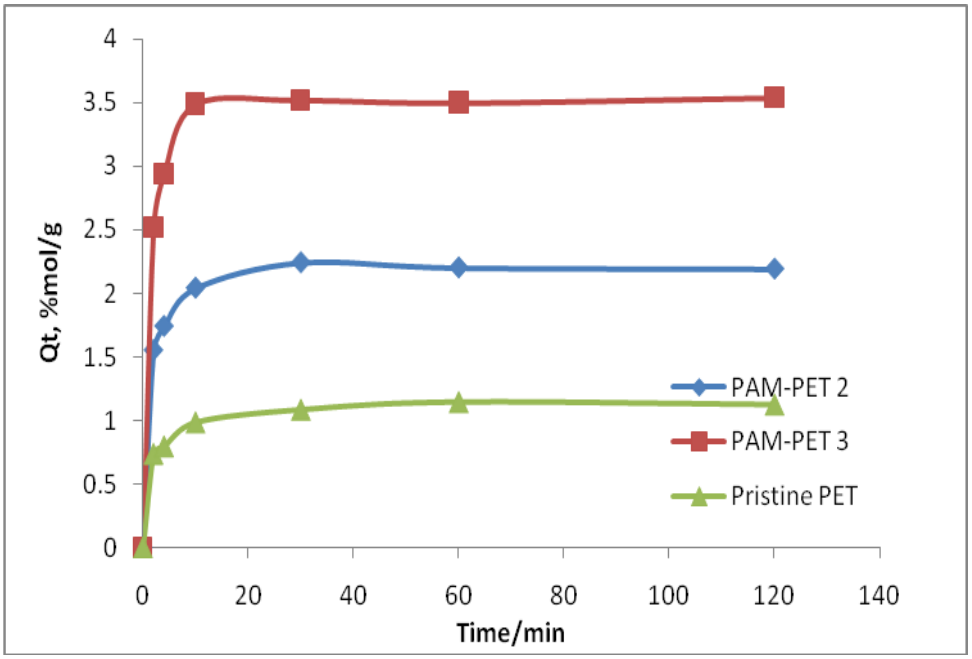

Figure 14 Swelling kinetics of PAM-PET fabric

In addition to the effective antibacterial properties, another favorable characteristic is achieved after the modification, quick swelling with water. This is majorly due to that PAM polymer network could work as responsive gel. This phenomenon also confirmed the formation of PAM network on the surface.

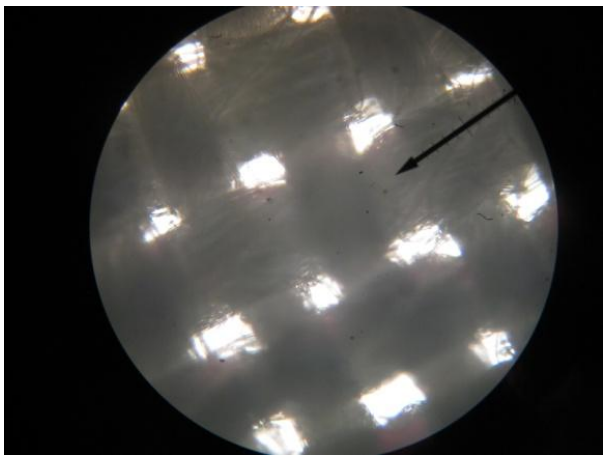
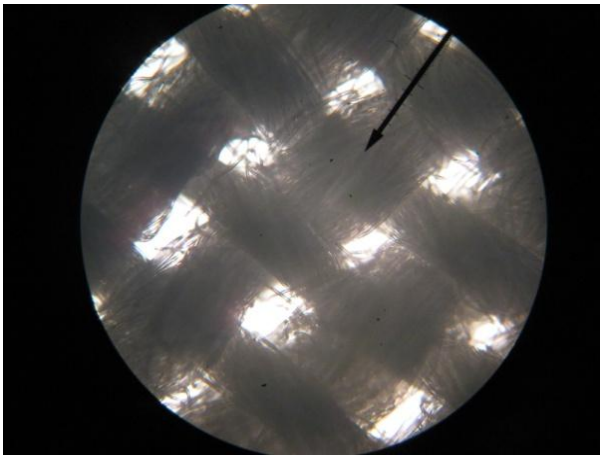

(a) PAM-PET 3 (immobilization percentage 21%), Pristine PET 0 min

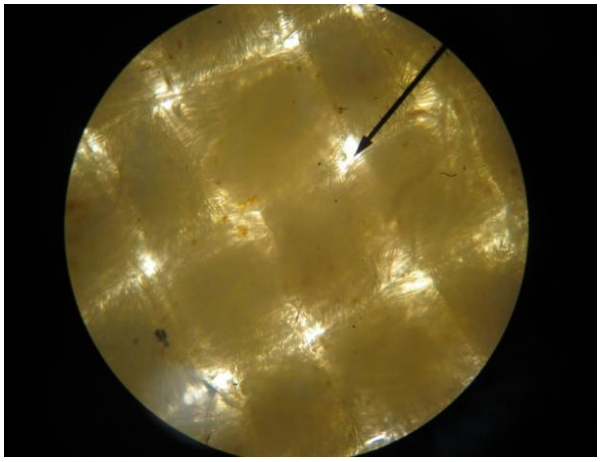
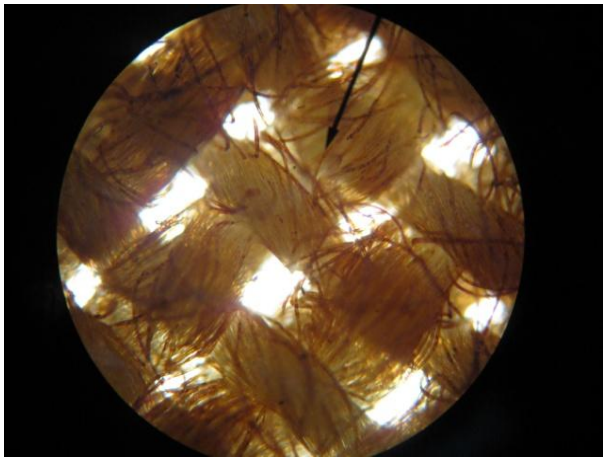

(b) PAM-PET 3 (immobilization percentage 21%), Pristine PET 4min

Figure 15 Microscopy images of swollen fabrics

The kinetics of the swelling process was investigated by means of the weight test at 20 ℃. After soaking in water for certain duration and centrifugation for 4 s to remove the attached water, the up-take of the fabrics was calculated. Swelling kinetics of PAM-PET is shown in Figure 15. The The up-take of water by the fabrics keeps increasing until the equilibrium is achieved. The equilibrium up-take increased as the IP increase. As shown in the figure, the swelling speed increase as the IP increase. The PAM-PET 3(IP=21%) could swell in 10 min. Pictures under microscopy (Figure 15) shows the responsive property of the PAM-PET.

Compared to pristine PET fabric, the modified PET could swell significantly in 4 min and block the spaces between yarns. So the modified fabric could perform a "smart" protection. Under normal conditions, immobilized polyacrylamide collapses to remain the porous structure and good breathability of the PET fabric. In contact with the biological fluids, polyacrylamide network responds by swelling. More insidious fluids can be blocked physically and the absorbed fluid will be decontaminated in situ. Finally dual protective functions are achieved in this way.

5.6 Regenerability study

After confirmation of the effective antibacterial performance and smart protective property of the PAM modified PET, we studied the regenerability of its antibacterial function in this paper. We investigated regenerability of the antibacterial performance of surface themoplastic IPN between PAM and PET with three different crosslinkers: MBA, divinylbenzene (DVB) and 2-ethyleneglycol diacrylate (EGDA) (PAM-PET-M, PAM-PET-D and PAM-PET-E), and studied the influence of the crosslinker on the properties of the treated fabrics,

5.6.1 Active chlorine regenerablity

The convenient, non-destructive and effective antibacterial modification on PET was achieved by forming a thermoplastic semi-IPN between PET and polyamide. Densities of functional groups introduced onto the PET surface by common radical grafting polymerization are generally less than 10×10^{-5} mol/g whereas the density of durable functional group of more than 100×10^{-5} mol/g could be achieved by forming a thermoplastic

semi-IPN on PET surface. (Bech, Meylheuc, Lepoittevin & Roger, 2007; Bech et al., 2009; Liu & Sun ,2008) The immobilized PAM on PET fabrics can be conveniently converted to acyclic N-halamine which has been confirmed as a biocide demonstrating potent antibacterial activities. The N-halamine is favoured as an antibacterial agent primarily due to its efficient antibacterial function and regenerable performance. So we investigated the regenerability of PAM-PET for 29 regeneration cycles.

In the regenerability test, the sample was treated with "chlorination-quench-chlorination"cycles. The amide modified samples were converted to halamine structures by immersing the samples in a diluted chlorine bleach solution (1500 ppm available chlorine) at room temperature for 30 min. The active chlorine was quenched in the titration process which was used to quantify the active chorine concentration on PAM-PET. The N-halamine structure could be regenerated from amide with another chlorination process.

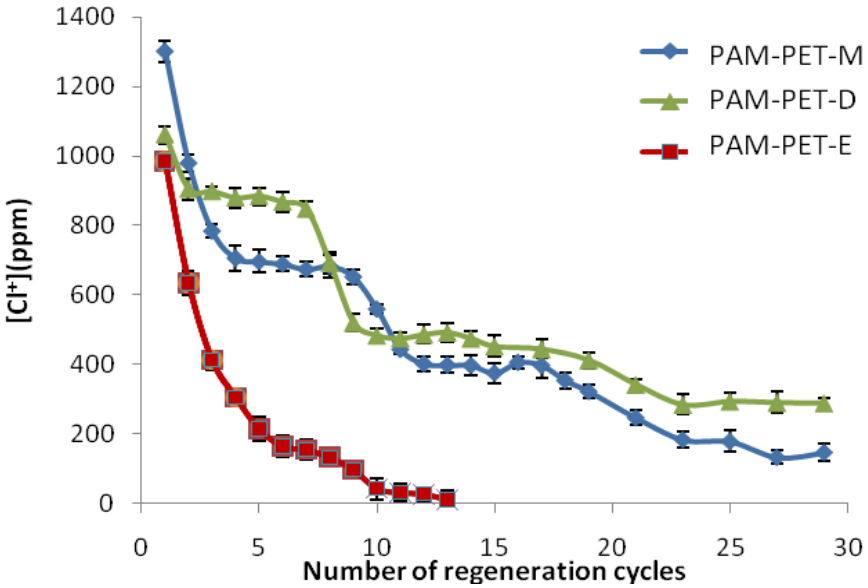

Figure 16 The active chlorine concentration [Cl^+] on PAM-PET versus number of regeneration cycles

The active chlorine contents on PAM-PET-M, PAM-PET-D and PAM-PET-E fabrics are plotted versus the regeneration cycles in Figure 16. With all these three crosslinkers, the achieved active chlorine decreased as the regeneration cycles increased. However, the performances of the PAM-PET crosslinked with different crosslinker are different. The N-halamine regeneration curve of PAM-PET-E presents a continueous drop of active chlorine till the 13th cycle where there is almost no active chlorine on the fabric. The regenerability evolutions of both PAM-PET-M and PAM-PET-D samples look similiar and can be devided into three stages based on the curve shapes. In the first several regeneration cycles, both samples show abrupt drops of active chlorine contents. Following that drop, there is a "psudo" stable stage. Suprisingly, there is another decrease after the first stable stage. Then, there is a more or less stable stage followed by another drop which is relatively less steep. Finally, the active chlorine stays constant on both sample.

5.6.2 Mechanism for the loss of regenerability

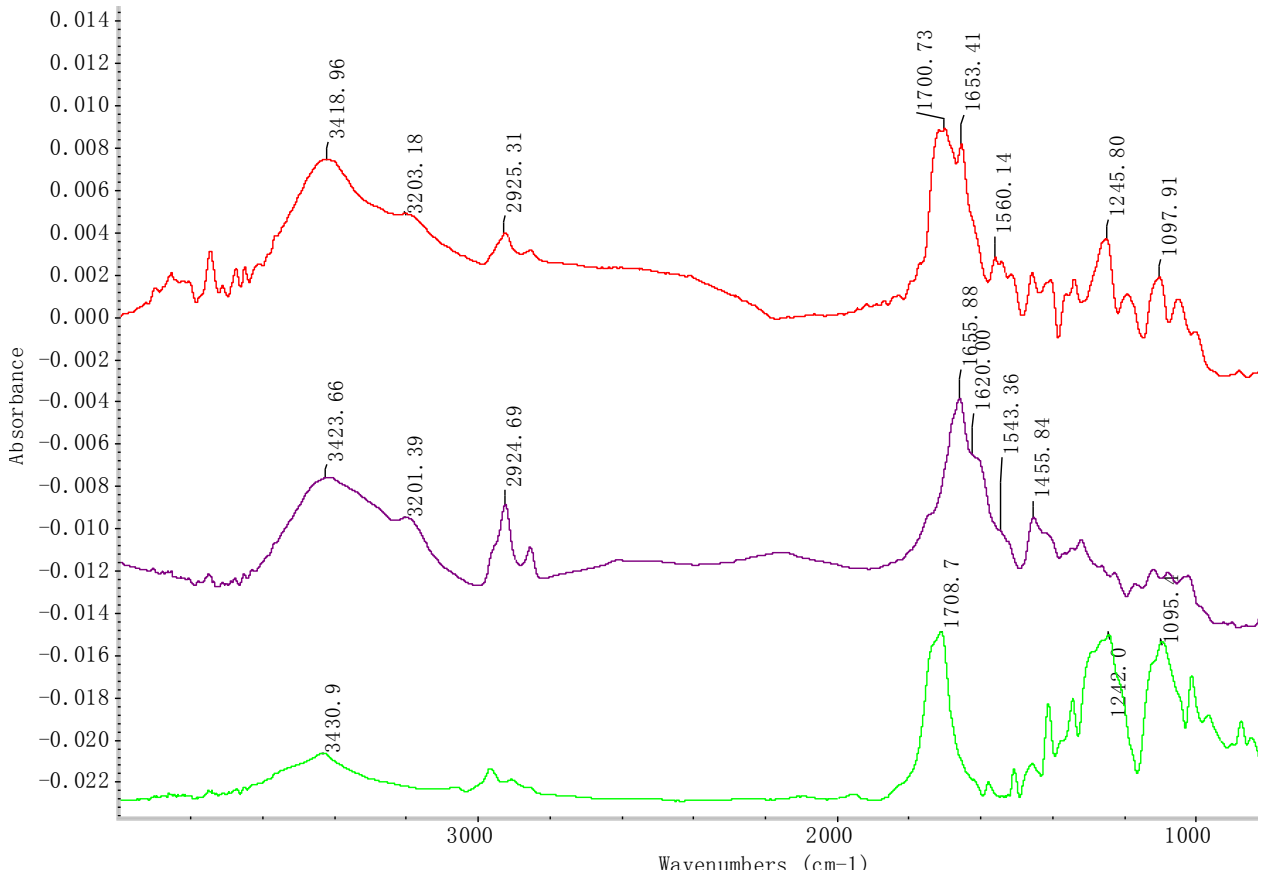

Figure 17 Subtracted FTIR spectra of a) PAM-PET-M after 2 regeneration cycles and pristine PET, b) PAM-PET-M with 0 regeneration cycles and pristine PET, and c) FTIR spectra of PET pristine

To find out the reasons for the degradation of N-halamine regenerability, FTIR , nitrogen content analysis, and acid group titration of the modified PET samples were employed in the study.

Figure 17 presents the subtracted FTIR spectrum (a) between PAM-PET-M after 2 regeneration cycles and PET pristine. After 2 regeneration cycles, besides the amide peak (1653cm^{-1}), a new peak at 1700 cm^{-1} attributed to carboxylic acid occurs in the subtracted FTIR spectrum, suggesting hydrolysis of the immobilized PAM. This is the reason for the

steep droping of active chlorine concentration on PAM-PET-M after the first several regeneration cycles. Since the PH of the chlorination solution is 11.4, alkaline hydrolysis of the immobilized amide structure to carboxylic acid could occur during the chlorination, leading to loss of chlorine binding sites on PAM-PET. According to previous studies(Kurenkov, Hartan & Lobanov, 2001; Nagase & Sakaguchi, 2003), alkaline hydrolysis of PAM proceeds even at a higher rate compared with low-molecular-weight amides because the carboxylate groups formed in hydrolysis accelerate the hydrolysis of the neighboring amide groups (anchimeric contribution).

Table 7 Contents of functional groups including [active chlorine], [amide group] and [acid group] on PAM-PET-M, PAM-PET-D and PAM-PET-E fabrics
a) The IP based on weight of PAM-PET-M, PAM-PET-D and PAM-PET-E are 13.17%, 13.25% and 13.21% respectively.

Regeneration cycles	PAM-PET-M [Cl]	[Amide group](N analysis)	[Acid groups] On fabric	PAM-PET-D [Cl]	[Amide group](N analysis)	[Acid groups] On fabric	PAM-PET-E [Cl]	pristine PET [Acid groups]
	ppm	1×10^{-7}mol/g	1×10^{-7} mol/g	ppm	1×10^{-7} mol/g	1×10^{-7} mol/g	ppm	1×10^{-7} mol/g
0	0	185.4	21.0	0	186.5	20.6	0	20.0
1	1302±30.2	168.8	_	1061±24.9	_	_	984±20.4	30.6
2	980±24.9	94.5	88.5	904±32.1	140.6	61.3	634±33.2	20.9
3	784±19.7	_	_	898±14.8	_	_	412±27.3	_
4	706±26.7	_	_	879±30.6	_	_	305±24.9	_
5	696±32.8	_	_	884±25.5	109.2	33.3	214±35.9	_
6	689±21.2	74.5	28.08	867±27.6	_	_	164±30.7	20.2
7	674±20.5	_	_	847±21.4	_	_	154±28.3	_
8	683±33.1	_	_	692±29.4	74.5	27.8	132±27.8	_
9	652±20.5	_	_	520±23.8	_	_	96±22.6	_
10	559±15.1	_	_	483±19.3	_	_	42±31.1	_
11	443±22.1	_	_	475±26.8	_	_	30±25.9	_
12	402±21.4	_	26.56	486±31.1	_	_	26±28	20.2
13	398±22.7	_	_	492±27.6	51.1	30.8	10±26.2	_
14	397±30.4	_	_	474±22.9	_	_	_	_
15	375±29.6	_	_	452±25.4	_	_	_	_
16	406±17	_	_	_	_	_	_	_
17	397±36.1	32.1	_	444±28.4	_	_	_	_
18	354±22.6	_	_	_	_	_	_	_
19	322±19.1	_	_	412±30.1	42.7	32.8	_	_
21	246±22.3	_	_	342±22.9	_	_	_	_
23	183±24.2	12.2	21.68	284±22.7	37.9	35.6	_	20.5
25	178±31.5	_	_	294±30.1	_	_	_	_
27	132±19.9	_	_	301±28.4	_	_	_	_
29	146±24.4	14.5	21.4	289±29.7	41.8	32.0	_	20.7

The finding that the amide structure was partially hydrolyzed into carboxylic acid during chlorination is also evidenced by the increase of carboxylic acid group quantity on fabric as shown in Table 7. Carboxylic acid group on PET fabrics was qunatified by a dye titration method. (Ivanov et al, 1996) Briefly, PET fabrics were allowed to interact with thionine

acetate in its aqueous solution for 10 hours. The amount of thionite acetate that was adsorbed onto the surface of PET fabrics via ionic bonding with carboxylic acid can be calculated based on the concentration difference of thionite acetate before and after the adsorption. The amount of carboxylic acid group on pristine PET is 20.0×10^{-7} mol/g. After 2 regeneration cycles, the number increases to 88.5×10^{-7} mol/g for PAM-PET-M, and to 61.3×10^{-7} mol/g for PAM-PET-D. Since nitrogen element only exists in the immobilized polymer network, nitrogen content can give an insight of the remaining IPN on PET. For PAM-PET-M, after 2 regeneration cycles, the lost nitrogen amounts to 90.9 $\times10^{-7}$mol/g ((185.4-94.5)$\times10^{-7}$mol/g). The increased carboxylic acid group equals to 67.4×10^{-7}mol/g ((88.5-21.0)$\times10^{-7}$mol/g) which is around 74.3% of the amount of lost nitrogen (or amide structure). It means around 25% of the nitrogen loss is due to the loss of interpenetrating network. This is because the crosslinker MBA also experiences hydrolysis during the chlorination, leading to the damage of the interlocking structure. However, applying the same analysis on PAM-PET-D, it is found that 92.7% of amide structure loss is due to hydrolysis of PAM amide and only around 7% is due to the the loss of interpentrating network. The much less amount of IPN damage in the case of PAM-PET-D is reasonable since the crosslinker DVB is nonhydrolyzable. Since the ester bond in the crosslinker EGDA is more susceptible to alkaline hydrolysis as compared to the amide bond in MBA, more severe loss of the IPN occurs (Figure 16) causing a quick decrease of active chlorine content with increase of the regeneration cycle.

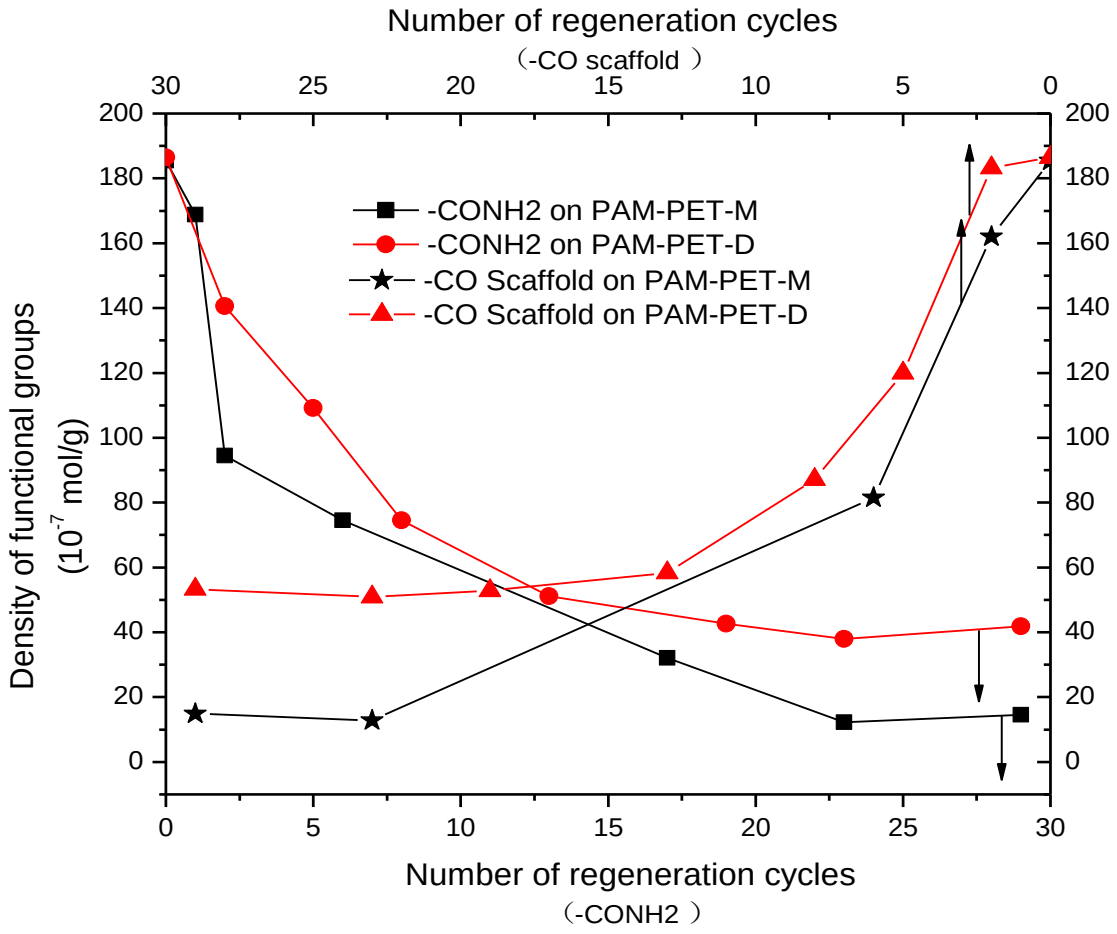

Figure 18 Amide content and C=O scaffold structure of PAM on PAM-PET as a function of the number of regeneration cycles

a) The density of $–CH_2–CH(CO)-$ scaffold struture on PAM-PET equals to the sum of density of $–CONH_2$ (N content) and –COOH density on hydrolyzed PAM network as shown in Table 7.

Nitrogen contents of both PAM-PET-M and PAM-PET-D were plotted against regeneration cycles in Figure 18 to present a clearer view of the trend of amide structure loss. The slope of amide structure loss decreases from cycle 2 to 23 for both samples. During these regeneration cycles, the electrostatic repulsion between the OH^- ions and the accumulating carboxylate anions ($–COO^-$) will decelerate the hydrolysis of amide. Even though there is a continueous decrease of nitrogen contents between 2-7 cycles for PAM-PET-D and 4-8 cycles for PAM-

PET-M, amounts of N-halamine structure (equivalent to [Cl^+]) keep essentially constant (Figure 2). Take PAM-PET-D for example, in 2-6 regeneration cycles, the loss of amide structure is due majorly to the loss of the immobilized IPN since the decrease of nitrogen content (from 140.6 to 109.2×10^{-7} mol/g) is accompanied by a simultaneous decrease of carboxylic acid group (from 61.3 to 33.3×10^{-7} mol/g). Peeling of the outermost immobilized PAM network exposes another layer PAM for chlorination, giving a "pseudo" stable active chlorine content ([Cl^+]).

However, loss of the immobilized IPN structure in the case of PAM-PET-D seems quite contradictory to the fact that DVB is nonhydrolyzable in the alkaline chlorination. So, surface carboxylic acid group of pristine PET was also analyzed by dye titration after it went through the same chlorination-quench cycles. As can be seen from the last column in Table 7, carboxylic acid group slightly increases after the first chlorination and then decreases indicating break down and dissolving of the PET polymer chain from the surface PET fabric. In the case of PAM-PET-D, due to the protection of the PAM network in the surface of modified PET, the hydrolysis of PET substrate primarily started after several regeneration cycles. The damage of surface PET resulted in the unlocking and loss of the immobilized PAM network. This explains the loss of PAM network in PAM-PET-D.

To better understand the status of the PAM network on PAM-PET, the contents of $–CONH_2$ and –COOH on PAM backbone can be added up to represent the content of total C=O or the CH2–CH(CO)- scaffold structure. The data are presented in Figure 18. After 13 regeneration cycles, there is almost no loss of PAM network on PAM-PET-D although very small

decrease of active chlorine concentration occurs due to further hydrolysis of amide. Nitrogen content and active chlorine value of both PAM-PET-D and PAM-PET-M keep essentailly constant in the end as shown in Figures 16 and 18. This is in consistent with the previous finding that hydrolysis of polyarylamide results BAB (B: -COOH A:-$CONH_2$) type structure and the formed carboxyl group can repel OH^- ions contributing to the stability toward further hydrolysis. (Kurenkov, Hartan & Lobanov, 2001; Nagase & Sakaguchi, 2003) Also, after the initial hydrolysis of surface PET polymer in amorphous area, there is no further hydrolysis of PET under the mild hydrolytic condition (room temperature, pH 11) as can be seen from the date in Table 3 (the last column).

5.6.3 Impact of the crosslinker on the N-halamine regenerability

The different crosslinker used in the preparation of PAM-PET results in the difference in surface network structure, durability of the network, swelling properties, and final amide structure retained. All of the factors will affect the final regenerated active chlorine concentration on the fabric and the final antibacterial performance. The difference in the evolvement of the active chlorine shown in Figure 17 also confirmed significant influence of the crosslinker on the chlorine regenerability. A lot of researchers had reported the hydrolysis of amide and ester structure in alkaline solution. (Heyman, 1982; Broxton & Duddy, 1981; Xiong & Zhan, 2006; Cheshmedzhieva et al., 2008; Bamford,1972) As shown in Scheme 3, the -C(O)-NH- in MBA and –C(O)O- in EGDA can also be hydrolyzed in the chlorination process at the same time with the hydrolysis of monomer amide structure. The hydrolysis speed of the crosslinkers EGDA> MBA> DVB is contrary to the speed of regenerability loss EGDA<MBA<DVB. Crosslinkers serve as key agent in the formation of the thermoplastic

semi-IPN. Once the crosslinker is hydrolyzed, the knot in the network will be lost and the network scaffold structure can be easily removed as shown in Scheme 3. The breakage of the crosslinker would cause significant loss of PAM network on PET surface and dramtically influence the regenerability of PAM-PET. The EGDA sample shows the best swelling properties but worst regenerability and durability as shown in Table 8. The quickest loss of the immobilized surface functional group is majorly due to the quickest hydrolysis of ester crosslinker. Meanwhile, the highly hydrophilic structure of EGDA renders it bad affinity to the hydrophobic polyester fiber and molecules. This will cause the smaller depth of EGDA diffusion into PET then result in the fact that most networks are embedded on the outermost surface and easily removed in the extraction and chlorination and titration cycles. So our study focuses on DVB and MBA samples.

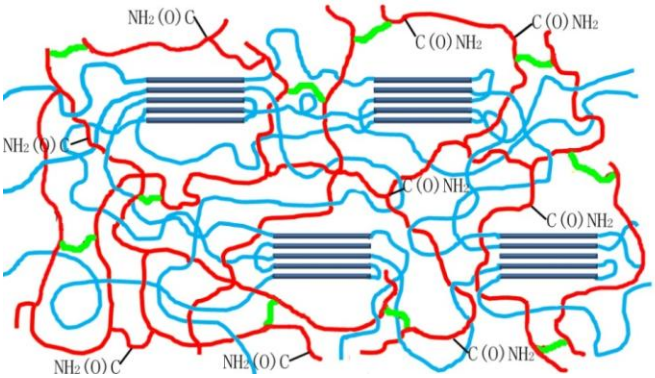

(a) Thermoplastic semi-IPN of PAM-PET-M

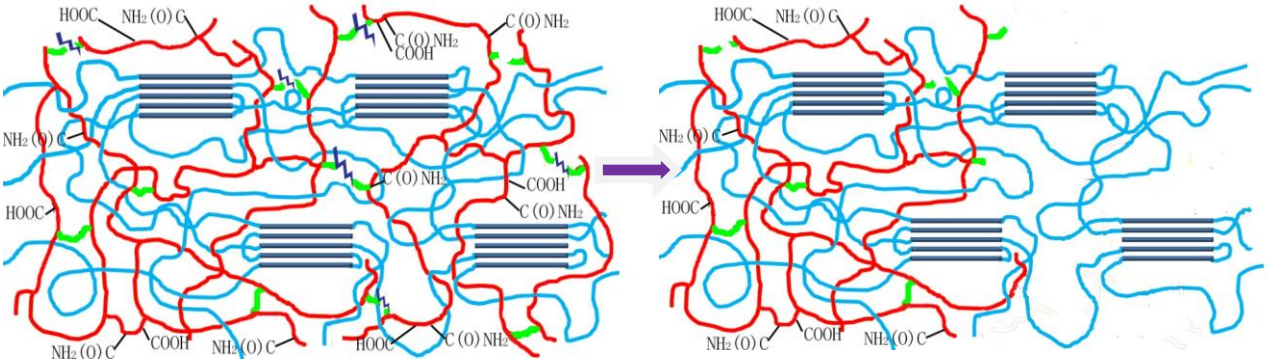

(b) Loss of the network scaffold as a result of the hydrolysis of crosslinker MBA in the network

Scheme 3 Schematic diagram of the mechanism of thermoplastic semi-IPN disintegration

Blue lines represent semicrystalline polymer network
Red lines represent crosslinked poly(acrylamide)
Green lines represent linkage formed by crosslinker MBA

Table 8 The swelling ratio of PAM-PET with different crosslinkers

Sample[a]	**PET**	**PAM-PET-M**	**PAM-PET-D**	**PAM-PET-E**
Swelling ratio[b]	1.15±0.01	1.30±0.02	1.31±0.02	1.49±0.01
Swelling ratio of the grafted PAM network	–	2.41±0.23	2.49±0.24	4.01±0.12

a) AM concentration 3 mol/l and BP 0.055 mol /L, and crosslinker/monomer ratio MBA/AM 1.5%, DVB/AM 1.1% and EGDA 5% ; The IP of the three samples are at 13.45±0.5%.
b) Swelling duration: 1 hour.

As presented in Figure 18, the content of total C=O or the CH_2–CH(CO)- scaffold structure on PAM-PET-D fabric after the first two regeneration cycles decreases only 2.79% which means that almost all of the -CH_2–CH(CO)- scaffolds are retained on PAM-PET-D after the first two cycles. However the network loss on PAM-PET-M samples is 12.6%, much bigger than PAM-PET-D. The scaffold structure of PAM-PET-D becomes stable after 13 cycles while PAM-PET-M does not stabillize until 23 cycles. After 30 regeneration cycles, the quantity of active chlorine on PAM-PET-D is almost 2 times of that on PAM-PET-M, and the residual –CH2-CH-C(O)- scaffold structure on PAM-PET-M is about 3 times of that on PAM-PET-M sample. In the end there is almost no acid groups left on PAM-PET-M sample, but there is still 7.1×10^{-6} mol/g on PAM-PET-D sample. Both the structure durability and final active chlorine concentration are better with crosslinker DVB. In the end, the antibacterial regenerability of PAM-PET can be improved with DVB since active chlorine concentrations (the amount of N-halamine structure) is closely related to antibacterial activities. This will be discussed in the following session.

5.6.4 The connection between active chlorine and antibacterial performance

N-halamine has favourable broad spectrum antibacterial activities. The previous study has reported the antibacterial performance of N-halamine structure converted from PAM immobilized PET (PAM-PET-M, [Cl^+]: 1403 ppm) against an antibiotic-resistant clinical isolate of hospital–associated methicillin-resistant *S. aureus* (HA-MRSA isolate #70527) following the modified AATCC test method 100–2004. The amide was converted to N-halamine in a chlorination process. The active chlorine on PAM-PET can be adjusted by the available chlorine concentration and chlorination duration in the chlorination process. By

studying the relationship between active chlorine and antibacterial activity, regenerability of the antibacterial activity on PAM-PET can be inferred.

In this study, the chlorinated PAM-PET-M, PAM-PET-D and PAM-PET-E samples (all with IP close to 13%) were all challenged by a HA-MRSA (isolate # 70527) following the modified AATCC test method 100–2004. The antibacterial activity of PAM-PET versus varying active chlorine concentrations was studied. The [Cl^+] value was adjusted by changing the available chlorine concentration of the chlorination solution. 5 min ultrasonic shaking was applied after the quench of the antimicrobial agent active chlorine to sufficiently release the bacteria attached on the fabric. Afterwards, the samples providing total eradication of bacteria were investigated with an agar incubution test to further confirm total kill.

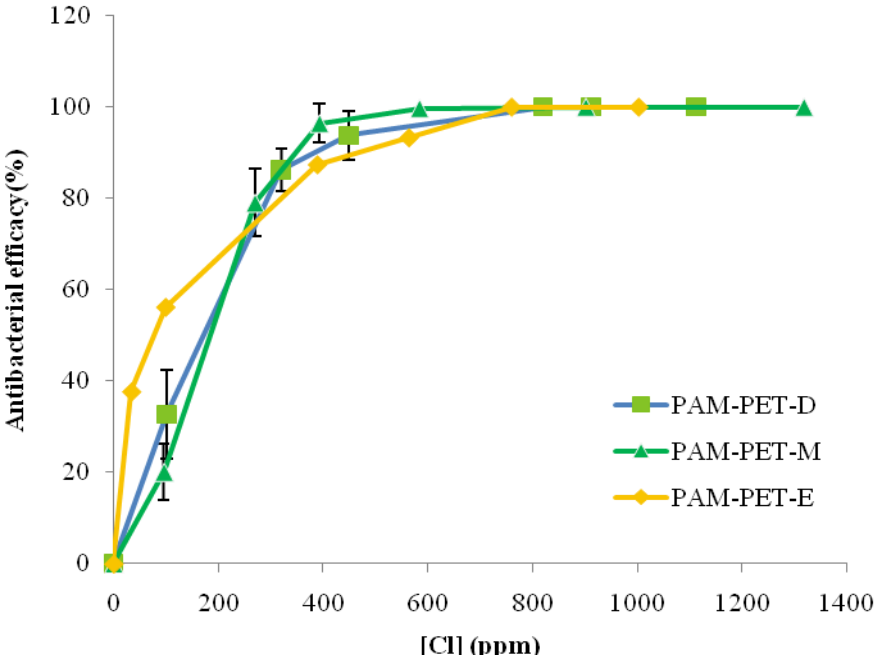

Figure 19 The relationship between antibacterial efficacy and active chlorine concentration on PAM-PET

a) The IP of PAM-PET-M, PAM-PET-D and PAM-PET-E fabrics are 13.3±1.4%, 12.9±1.52% and 13.2±1.62% respectively.

Figure 19 presents the relationship between antibacterial activity and active chlorine quantity on PAM-PET-M, PAM-PET-D and PAM-PET-E. The kill ratio of the N-halamine increased as the applied biocidal stress ($[Cl^+]$). Because the initial bacterial quantity challenged by the modified fabric is definite, the kill ratio in established time represents the relative inactivation rate of the N-halamine structure. So the trend indicates the inactivation rate keeps increasing as N-halamine concentration rises.

All the PAM-PET-M, PAM-PET-D and PAM-PET-E samples showed efficient antibacterial performance. No bacterial colonies could be observed even after 48 hours of culture on any agar plates contacted with PAM-PET-M and PAM-PET-D samples which suggests total bacterial killing after the antibacterial test. This proves antibacterial acitivity results of PAM-PET-M and PAM-PET-D are credible and the total kill is a "real and true" finding. However, in the case of PAM-PET-E, several colonies were observed on the agar plate after 48 hours incubation. This indicates that the antibacterial activity of PAM-PET-E samples were overestimated in Figure 5. This is due to the quick swelling of the PAM-PET-E fabric and the 5 min ultrasonic shaking couldn't adequately extract the absorbed bacteria out of the PAM-PET-E fabric. The swelling ratio of PAM-PET-E is much higher than that of the other two PAM-PET-M and PAM-PET-D as shown in Table 8. It could carry out rapid absorption of bacterial solution and traped the live bacteria in the PAM network. This is also why the PAM-PET-E samples demonstrate nominally "better" antibacterial efficacies than the other two samples when the active chlorine concentration is smaller than 300ppm (Figure 19). So the results of the PAM-PET-E sample should be discounted. The following discussion will primarily focus on antibacterial activities of PAM-PET-M and PAM-PET-D samples.

The relationship between antibacterial activity and active chlorine quantity on PAM-PET-M, PAM-PET-D and PAM-PET-E is shown in Figure 19. The kill ratio of the N-halamine increased as the applied biocidal stress which is the increasing active chlorine concentration. Because the initial bacterial quantity challenged by the modified fabric was definite, the kill ratio in established time represents the relative inactivation rate of the N-halamine structure. So the trend indicates the inactivation rate keeps increasing as N-halamine concentration rises.

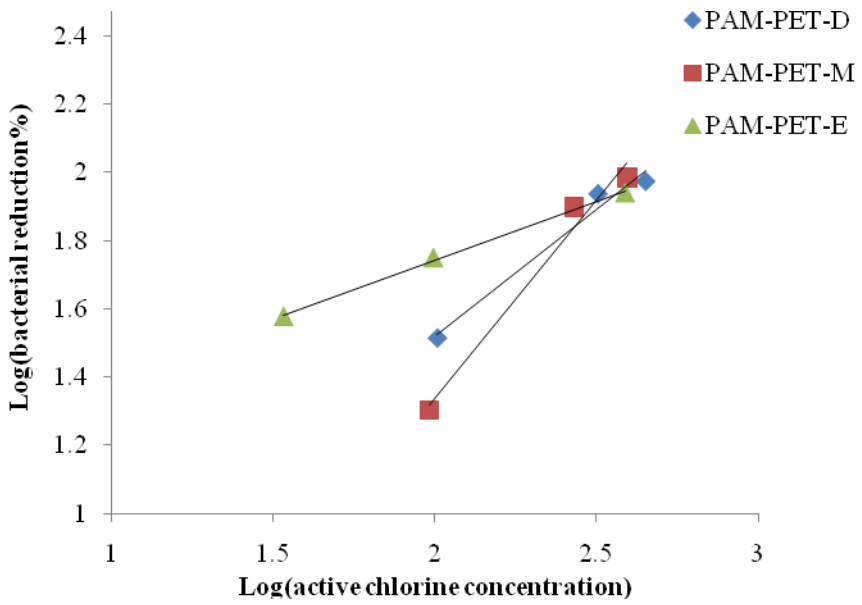

Figure 20 Log of bacterial reduction percentage versus log of concentration of antibacterial agent active chlorine [Cl^+]

As shown in the Figure 19, concentration of the biocide affects the lethal activity significantly. The relationship between the logarithm of bacterial reduction ratio in 10 min and active chlorine concentration was ploted in Figure 20. Hurwitz et has reported that the concentration of the biocide and respective time needed for the certain degree of inactivation follows: (Russell, 2004)

$C_1^{\eta}t_1 = C_2^{\eta}t_2$

The concentration exponent η is the measure of the effect of the changes in biocide concentration on cell death rate.

$$\eta=(\log t_2-\log t_1)/(\log C_2-\log C_1) \quad (11)$$

In Figure 20, the logarithm of bacterial reduction and active chlorine concentration show a good linear relationship. The slope equals to the concentration exponent of N-halamine. As can be seen from Figure 20, the η values of chlorinated PAM-PET fabrics are all smaller than 2. It was reported that those biocides with η values smaller than 2 interacted with their target by chemical or ionical binding (Hugo & Denyer, 1987). This result confirms that N-halamine functions as an oxidizing agent in destroying the cellular activity of protein(Bloomfield,1996; Dennis, Olivieri & Kruse, 1979; Williams, Swango, Wilt, Worley, 1991; Elder & Worley, 1988).The smaller η values as compared with various other biocides such as aliphatic and aromatic alcohols, phenolics and sorbic acid means the antibacterial activity of the N-halamine is less dependent on its concentration. This enables N-halamine modified PET to maintain an effective antibacterial activity even after many regeneration cycles.

As reported the effective biocidal action needs contact interaction of the biocide with the target site and the accumulation of the biocides to the damage level. (Denyer, 1995) So on the typical line of percent loss of bacterial viability versus applied biocidal stress there is a initiation stage when the bactericidal effect is reversable for the unsufficient biocidal concentration (Denyer, Stewart, 1998). However this stage was not obvious shown on Figure

19. After initiation stage, the biocidal effect of antibacterial agents as N-halamine which has an effect on metabolic activity could be supplemented by a autocidal activity resulted by the free radical accumulation through metabolic imbalance. (Phillips-Jones & Rhodes-Roberts, 1991) The autocidal effect leads to the self-destruction of bacteria and accounts for the significant proportion of population death and auto-acceleration phenomenon in the second stage as shown Figure 19 before total kill. It initiates the transition of sub-lethal damage of bacteria to cell death. Finally irreversible total bactericidal effect is caused by high biocidal concentration. The characteristics of the first two stages could be influenced by the physicochemistry of N-halamine because that the biocide physicochemistry could effect the efficacy of target interaction. So besides chemical properties both the steric hinderence of N-halamine monomer and network structure of immobilized modification network can siginificantly influence the accessibility of the bicide to the bacterial cell. This will be studied in future work.

5.6.5 The antibacterial regenerability

The antibacterial regenerability of PAM-PET fabrics after different regeneration cycles could be inferred by correlating their active chlorine concentration (Table 7) with antibacterial activities according to the curves in Figure 19. It is showed that PAM-PET-M could provide a total kill of 10^6 CFU/ml HA-MRSA within 10 minutes after the second regeneration cycle ($[Cl^+]$ = 980 ppm) and >99.7% reduction after the 9th regeneration cycle ($[Cl^+]$ = 652 ppm). Also, the effective total inactivation activity of HA-MRSA by PAM-PET-D could sustain 7 regeneration cycles ($[Cl^+]$ = 847 ppm). However, PAM-PET-M after 29 regeneration cycles with 123±32 ppm active chlorine can only inactivate 20.1% of the bacterium in 10 minutes.

In the case of PAM-PET-D, even after 29 regeneration cycles, 306±20 ppm active chlorine remaining on the sample can provide 86% kill of 10^6 CFU/ml HA-MRSA in 10 min, and 100% kill in 20 min (datum is not include in Figure 19).

Chapter 6: Conclusions and future work

The surface chemical inert PET was modified with a novel method via forming surface thermoplastic semi-IPN. Successful immobilization of PAM/PMAM was confirmed by FTIR and XPS. The thermoplastic semi-IPN is durable to Soxhlet extraction with both DI water and methanol. After being converted to N-chloramide structure, the PAM-PET fabric can demonstrate total kill of 10^5-10^6 CFU/ml healthcare-associated methicilin-resistant *Staphylococcus aureus* (HA-MRSA) isolate #70527, CA MRSA community associated methicilin-resistant *Staphylococcus aureus* (CA-MRSA) isolate #40065, *Staphylococcus aureus* isolate ATCC# 25923 , multidrug resistant extended spectrum *beta - lactamase* (MDR ESBL) isolate #70094 and multidrug-resistant *Pseudomonas aeruginosa* (MDR P. Aeruginosa) at the contact time of 15 minutes. Surface morphology of the fabrics did not show significant change after modification until the immobilization percentage exceeded 20%. The quantity of N-halamine on polyester is controllable. The vapour permeability keeps essentially the same after the surface modification while the air permeability shows slightly decrease. Analysis of the regenerability of PAM-PET-M, PAM-PET-D and PAM-PET-E in 30 "titration-chlorination regeneration" cycles by FTIR, element analysis and surface -COOH group titration showed that the degradation of regenerability was due to hydrolysis of acrylamide, crosslinkers and bulk pristine PET in chlorination process. The types of crosslinker influenced the regenerability significantly. Adopting divinylbenzene (DVB) as the crosslinker improved the antibacterial regenerability successfully. For the first 7 regeneration cycles, the sample demonstrated complete bacterial eradication within 10 min. Even after 30 regeneration cycles, the PAM-PET-D sample still resulted in a 100% reduction of 10^6 CFU/ml HA-MRSA within 20 min contact. In addition, the modified fabric could also

respond to water and swell in less than 10min. So the modified fabric could perform a "smart" protection.

The new modification technique by forming thermoplastic semi-IPN theoretically could be applied to several other different semicrystalline thermoplastic polymers surfaces such as PP and PU. Furthermore, other surface functions to fulfill certain application requirements should also be achieved by immobilizing different monomer precursors in this way. So there could be extensive applications of the method on different substrates to add interesting functions. In the future, the immobilization of several different functional monomers on chemically inert semicrystalline polymer surfaces by forming thermoplastic semi-IPN could be studied. At the same time, the functional modification by forming thermoplastic semi-IPN on different substrates such as PET, PP and PU film surfaces could also be studied.

References

Aizenshtein, E. M. (2007) World production and consumption of polyester fibres and yarn. *Fibre Chemistry*, 39, 355-362.

Altin, S., Altin, A., Elevli, B., Cerit O. (2003) Determination of Hospital Waste Composition and Disposal Methods: a Case Study. *Polish Journal of Environmental Studies*, 12, 251.

Bamford C.H. Ester formation and hydrolysis and related reactions. Amsterdam: Elservier Publishing Company, 1972.

Barner-Kowollik C., Vana P., Davis T.P. (2002) The kinetics of Free-Radical Polymerization. In: Matyjaszewski K, Davis T.P., editor. Hoboken N.J., p.187.

Baselga J, Llorente M.A., Hernandez-Fuentes I, Pierola I.F., (1989). Polyacrylamide networks: sequence distribution of crosslinker. *European Polymer Journal* 25(5): 477-80.

Bech L, Elzein T, Meylheuc T., Ponche A, Brogly M.E., Roger L.P. (2009) Atom transfer radical polymerization of styrene from different poly(ethylene terephthalate) surfaces: Films, fibers and fabrics. *European Polymer Journal*. 45 (1): 246-255.

Bech L., Meylheuc T.B., Lepoittevin B., Roger P. (2007) Chemical surface modification of poly(ethylene terephthalate) fibers by aminolysis and grafting of carbohydrates. *Journal of Polymer Science. Part A, Polymer Chemistry*. 45 (11): 2172-2183.

Bender, W, Peter, S. (2001) Antimicrobials for synthetic fibers. in "Bioactive Fibres and Polymers", Edwards, J. V., and Vigo, T. L. (eds), American Chemical Society, Washington DC, 2001, Ch. 13, 218-241.

Best, M., V. S. Springthorpe, and S. A. Sattar. (1994). Feasibility of a combined carrier test for disinfectants: studies with a mixture of five types of micro-organisms. *American Journal of Infection Control* , 22,152-162.

Billovits G.F., Durning C. J., (1988) *Polymer 29,* 1468.

Bloomfield, S. F. (1996). Chlorine and iodine formulations, p. 133-158. In J. M. Ascenzi (ed.), Handbook of disinfectants and antiseptics. Marcel Dekker, Inc., New York, N.Y.

Bloomfield, S. F. and Arthur M. (1992). Interaction of Bacillus subtilis spores with sodium hypochlorite, sodium dichloroisocyanurate and chloramine-T. *Journal of Applied Bacteriology*. 72,166-172.

Bloomfield, S. F., Smith-Burchnell, C. A., and Dalgleish A. G. (1990). Evaluation of hypochlorite-releasing disinfectants against the human immunodeficiency virus (HIV). *Journal of Hospital Infection*, 15,273-278.

Broxton T.J, Duddy N.W. (1981) Hydrolysis of esters and amides in strongly basic solution. Evidence for the intermediacy of carbanions. *J. Org. Chem.* 46 (6): 1186–1191.

Caykara T., Turan E. (2006) Effect of the amount and type of the crosslinker on the swelling behavior of temperature-sensitive poly(N-tert-butylacrylamide-co-acrylamide) hydrogels. *Colloid and Polymer Science*. 284: 1038–1048.

Cheshmedzhieva D, Ilieva S, Hadjieva B, Galabov B*, (2008) The mechanism of alkaline hydrolysis of amides: a comparative computational and experimental study of the hydrolysis of N-methylacetamide, N-methylbenzamide, and acetanilide. *Journal of Physical Organic Chemistry* 22 (6): 619 – 631.

Chou, P. T., Cao, G., (2003). Adhesion of Sol-Gel-Derived Organic-Inorganic Hybrid Coatings on Polyester. *Journal of Sol-Gel Science and Technology* 27, 31–41.

Chun H.J., Cho S.M., Lee Y.M., Lee H.K., Suh T.S. (1999). Graft copolymerization of mixtures of acrylic acid and acrylamide onto polypropylene film. *Journal of Appllied Polymer Science*, 72, 251–6.

Cireli A., Kutlu B., Mutlu M., (2007). Surface Modification of Polyester and Polyamide Fabrics by Low Frequency Plasma Polymerization of Acrylic Acid, *Journal of Applied Polymer Science*, 104, 2318–2322.

Decker, C. Handbook of Polymer Science and Technology, (1989) vol. 3, p. 541.

Decker C, Zahouily K. (1998) Light-stabilization of polymeric materials by grafted UV-cured coatings. *Journal of Polymer Science Part A: Polymer Chemistry*, 36,2571–80.

Deng J.P., Yang W.T., Rånby B. (2000) Surface photografting polymerization of vinyl acetate (VAc), maleic anhydride (MAH), and their charge transfer complex. I. VAc(1). *Progress in Polymer Science*, 77,1513–21.

Deng J.P., Yang W.T., Rånby B. (2000) Surface photografting polymerization of vinyl acetate (VAc), maleic anhydride (MAH), and their charge transfer complex. II. VAc(2). *Progress in Polymer Science*, 77,1522–31.

Deng J.P., Yang W.T., Rånby B. (2000) Surface photograft polymerization of vinyl acetate on low density polyethylene film. Effects of solvent, *Polymer Journal*, 32,834–7

Deng J. P., Wang L. F., Liu L. Y., Yang W. T., (2009). Developments and new Applications of UV-induced surface graft polymerizations, *Progress in Polymer Science*, 34, 156-193.

Dennis, W. H., Olivieri, V. P. , and Kruse C. W. (1979) The reaction of nucleotides with aqueous hypochlorous acid. *Water Research*. 13, 357-362.

Denyer S.P., (1995) Mechanisms of action of antibacterial biocides. *Int Biodeterior Biodegrad*, 36: 227–245.

Denyer S.P., Stewart G.S., (1998) Mechanisms of action of disinfectants. *Int Biodeterior Biodegrad* , 41(3-4): 261-268.

Diaz , L. F., Eggerth, L. L., Enkhtsetseg , Sh., Savag, G. M. (2008) Characteristics of healthcare wastes. *Waste Management*, 28, 1219.

East, A. J. (2005) Polyester fibers, in "Synthetic fibers: nylon, polyester, acrylic, polyolefin", Mclntyre, J. E., The Textile Institude, Washington DC, Ch. 3, pp. 95-141.

Gabbay, J., Borkow, G., (2006).Copper Oxide Impregnated Textiles with Potent Biocidal Activities, *Journal OF Industrial Textiles*, 35, 4,323.

Gnanou, Y. (2008) Organic and physical chemistry of polymers, p.302.

Hamoda, H. M., El-Tomi, H. N., Bahman, Q. Y. (2005) Variations in Hospital Waste Quantities and Generation Rates. *Journal of Environmental Science and Health*, A40:467–476.

Gregory, J. G., Ahmad E. Madkour, T. E., Gregory N. T. (2007). Infectious disease: Connecting innate immunity to biocidal polymers. *Materials Science and Engineering*, 57(R), 28-64.

Heyman E. Hydrolysis of carboxylic esters and amides. In: Jakoby W.B., Bend J.R., Caldwell J, editors., New York: Ac-ademic Press, 1982. p229-245.

Hsieh, S. H., Huang, Z. K., Huang, Z. Z., and Tseng, Z. S., (2004) Antimicrobial and Physical Properties of Woolen Fabrics Cured with Citric Acid and Chitosan, *Journal of Applied Polymer Science* 94, 1999–2007.

Hugo W.B, Denyer S.P. The concentration exponent of disinfectants and preservatives (biocides) In: Board RG, Allwood MC, Banks JG, editors. Oxford: Blackwell Scientific Publications, 1987, 281–291.

Ivanov, V. B. ; Behnisch, J.; Holländer, A.; Mehdorn, F.; Zimmermann, H. Surf Interface Anal, (1996). 24, 257.

Joiner, B. G.,(2001) Determining Antimicrobial Efficacy and Biocompatibility of Treated Articles using Standard Test Methods, in "Bioactive Fibres and Polymers", Edwards, J. V., and Vigo, T. L. (eds), American Chemical Society, Washington DC, Ch. 12, pp. 201–217.

Kenawy, E., Worley, S. D., and Broughton, R. (2007). The Chemistry and Applications of Antimicrobial Polymers: A State-of-the-Art Review, *Biomacromolecules*, 8 (5), 1359-1384.

Kim, Y. H., and Sun, G., (2001). Durable Antimicrobial Finishing of Nylon Fabrics with Acid Dyes and a Quaternary Ammonium Salt, *Textile Research Journal*, 71, 318–323.

Kulikovsky, A., H. S. Pankratz, and H. L. Sadoff. (1975) Ultrastructural and chemical changes in spores of Bacillus cereus after action of disinfectants *Journal of Applied Bacteriology*. 38, 39-46.

Kurenkov V.F., Hartan H-G, Lobanov F.I. (2001) Alkaline Hydrolysis of Polyacrylamide. *Russian Journal of Applied Chemistry*. 74 (4): 543-554.

Lee, H. J., Yeo, S. Y, and Jeong, S. H. (2003) Antibacterial Effect of Nanosized Silver Colloidal Solution on Textile Fabrics, *Journal of Material Science*, 38, 2199–2204.

Rinaudo, M., (2006). Chitin and Chitosan: Properties and Applications, *Progress of Polymer Science*, 31, 603–632.

Lim, S. H., and Hudson, S. M., (2003). Review of Chitosan and its Derivatives as Antimicrobial Agents and Their uses as Textile Chemicals, *Journal of Macromolecule Science. Polymer Review.*, 43, 223–269.

Liu, S., Sun, G. (2006). Durable and Regenerable Biocidal Polymers: Acyclic N-Halamine Cotton Cellulose. *Industry Engineer Chemistry Research*, 45, 6477-6482.

Liu, S., Sun, G. (2008). Functional modification of poly(ethylene terephthalate) with an allyl monomer: Chemistry and structure characterization. *Polymer*, 49, 5225–5232.

Liu, S., Sun, G. (2009). New Refreshable N-Halamine Polymeric Biocides: N-Chlorination of Acyclic Amide Grafted Cellulose. *Industry Engineer ChemistryResearch*, 48, 613–618.

Liu S., Zhao N., Rudenja S, (2009) Surface Interpenetrating Networks of Poly(ethylene terephthalate) and Polyamides for Effective Biocidal Properties. *Macromolecular Chemistry and Physics*. 211: 286-296.

Louati, M., Elachari, A., Ghenaim, A., and Caze, C., (1999). Graft Copolymerization of Polyester Fibers with a Fluorine-Containing Monomer. *Textile Research Journal*, 69, 381.

Majumdar, P., Lee, E., Gubbins, N., Stafslien S. J., Daniels, J, Thorson, C. J. , Chisholm, B. J. (2009). Synthesis and antimicrobial activity of quaternary ammonium-functionalized POSS (Q-POSS) and polysiloxane coatings containing Q-POSS, *Polymer*, 1(9), 0032-3861

McDonnell, G., and Russell, A. D., (1999). Antiseptics and Disinfectants: Activity, Action, and Resistance, *Clinical Microbiol Review*., 12, 147–179.

Millar, M. R., Brown, N. M., Tobin, G.W., Murphy, P. J., Windso/r, A.C.M, Speller, D.C.E. (1994). Outbreak of infection with penicillin-resistant Streptococcus pneumoniae in a hospital for the elderly. *Journal of Hospital Infection.* 27, 99-104.

Nagase K, Sakaguchi K. (2003) Alkaline hydrolysis of polyacrylamide. *Journal of Polymer Science Part A: General Papers*. 3(7): 2475 – 2482.

Neely, A. N. (1999). Antimicrobial resistance. *Burns*, 25 17-24.

Neely, A. N. (2000). A survey of Gram-negative bacteria survival on hospital fabrics and plastics. *Journal of Burn Care Rehabilition.* 21,523.

Neely, A. N., Maley, M. P. (2000). Survival of enterococci and staphylococci on hospital fabrics and plastic. *Journal of Clinical Microbiol.* 38,724.

Neely, A. N., Orloff, M. M. (2001). Survival of Some Medically Important Fungi on Hospital Fabrics and Plastics. *Journal of Clinical Microbiol.* 39,3360.

Pan B, Viswanathan K, Hoyle C.E., Moore R.B. (2004) Photoinitiated grafting of maleic anhydride onto polypropylene. *Journal of Polymer Science Part A: Polymer Chemistry*, 42,1953–62.

Pascal P, Winnik M.A. *(*1993) Pulsed laser study of the propagation kinetics of acrylamide and its derivatives in water. *Macromolecules*. 26 (17): 4572–4576.

Phillips-Jones M.K., and Rhodes-Roberts M.E. Studies of inhibitors of respiratory electrontransport and oxidative phosphorylation In: Denyer SP, Hugo WB, editors. London: Academic Press, 1991. p. 203-224.

Purwar, R., and Joshi, M. (2004). Recent Developments in Antimicrobial Finishing of Textiles—A Review, *AATCC Review*, 4, 22–26.

Ren, X., Kocer H. B., Kou L., Worley, S. D., Broughton, R. M. , Tzou, Y. M., Huang, T. S. (2008), Antimicrobial Polyester, *Journal of Applied Polymer Science*, 109, 2756–2761

Rochery, M., Vroman, I. and Campagne, C., (2006). Poly(dimethylsiloxane and Poly(tetramethylene oxide)-based Polyurethane, *Journal OF Industrial Textiles*, 35(3), 227.

Russell A.D. Factors influencing the efficacy of amtimicrobial agents In: Fraise A.P, Lambert PA, Maillard J-Y, editors. Wiley-Blackwell, 2004, 104.

Sabour, M. R., Mohamedifard, A., Kamalan, H. (2007) A mathematical model to predict the composition and generation of hospital wastes in Iran. *Waste Management*, 27, 584.

Shih, K. L., and Lederberg, J. (1976) Effects of chloramine on Bacillus subtilis deoxyribonucleic acid. *The Journal of Bacteriology*. 125, 934-945.

Song, Y.-W. (2006). Effect of grafting of acrylic acid onto PET film surfaces by UV irradiation on the adhesion of PSAs, *Journal of Adhesion Science and Technology*, 20(12), 1357–1365.

Son, Y. A., and Sun, G., (2003). Durable Antimicrobial Nylon 66 Fabrics: Ionic Interactions with Quaternary Ammonium Salts, *Journal of Applied Polymer Science*, 90, 2194–2199.

Sun G. (2001) Durable and Regenerable Antimicrobial Textiles. in "Bioactive Fibres and Polymers", Edwards, J. V., and Vigo, T. L. (eds), American Chemical Society, Washington DC, 2001, Ch. 14, pp. 243-252.

Sun, G., Xu, X., Bickert, J. R., Williams, J. F. (2001) Durable and regenerable antibacterial finishing of fabrics with a new hydantoin derivative. *Industry Engineer Chemistry Research,* 40, 1016–1021.

Sun, Y. Y., Chen, T., Worley, S. D., Sun, G. (2001) Novel refreshable N-halamine polymeric biocides containing imidazolidin-4-one derivatives. *Journal of Polymer Science, Part A: Polym*er *Chemistry*, 39, 3073–3084.

Taylor, G. R., and M. Butler. (1982) A comparison of the virucidal properties of chlorine, chlorine dioxide, bromine chloride and iodine. *The Journal of Hygiene*. 89,321-328.

Williams, J. F., Cho, U. (2005). Antimicrobial Functions for Synthetic Fibers: Recent Developments, *AATCC Review*, 5, 17–21.

Worley, S. D.; Williams, D. E. (1998) Halamine water disinfectants. *CRC Critical Review of Environmental Control*, 18, 133–175.Yang, S. C., Kim J. P. (2008). Flame Retardant Polyesters. III. Fibers, *Journal of Applied Polymer Science*, 108, 2297-2300.

Williams D. E., Elder E. D., Worley S. D. (1988) Is free chlorine necessary for disinfection? *Applied and Environmental Microbiology*. 54, 2583–2585.

Williams D. E., Swango L. J., Wilt G. R., Worley S. D. (1991) Effect of organic N-halamines on selected membrane functions in intact Staphylococcus aureus cells. *Applied and Environmental Microbiology*. 57,1121–1127.

Xiong Y, Zhan C-G. (2006) Theoretical studies of the transition state structures and free energy barriers for base-catalyzed hydrolysis of amides*The Journal of Physical Chemistry . A*,

Zhao B., Brittain W.J. (2000) Polymer brushes: surface-immobilized macromolecules. *Progress in Polymer Science*, 25,677–710.

Zhong X.D., Ishifune M., Yamashita N., *(*2000) Study on copolymerization of Acrylamide with Styrene Initiated by Methyl Ethyl Ketone and its Derivatives in Comparision with conventional Radical Initiator, *Journal of Macromolecular Science*. A37(1&2): 49-63.